



FEDERAL UNIVERSITY OF SANTA CATARINA  
TECHNOLOGY CENTER  
GRADUATE PROGRAM IN CHEMICAL ENGINEERING

Rodrigo Botinelly Nogueira

Green synthesis of silver nanoparticles  
using extract of seed skins of guaraná (*Paullinia cupana*)

Florianópolis

2022

Rodrigo Botinelly Nogueira

Green synthesis of silver nanoparticles  
using extract of seed skins of guaraná (*Paullinia cupana*)

Dissertation presented to the Graduate Program in Chemical Engineering of the Federal University of Santa Catarina to obtain the Master of Science degree in Chemical Engineering.

Supervisor: Dachamir Hotza, Prof. Dr.

Co-supervisor: Lizandro Manzato, Prof. Dr.

Florianópolis

February 2022

Ficha de identificação da obra elaborada pelo autor,  
através do Programa de Geração Automática da Biblioteca Universitária da UFSC.

Nogueira, Rodrigo

Green synthesis of silver nanoparticles using extract  
of seed skins of guaraná (Paullinia cupana) / Rodrigo  
Nogueira ; orientador, Dachamir Hotza, coorientador,  
Lizandro Manzato, 2022.

86 p.

Dissertação (mestrado) - Universidade Federal de Santa  
Catarina, Centro Tecnológico, Programa de Pós-Graduação em  
Engenharia Química, Florianópolis, 2022.

Inclui referências.

1. Engenharia Química. 2. Nanotecnologia. 3. Síntese  
Verde. 4. Planejamento Experimental de Taguchi. 5.  
Atividade antibacteriana . I. Hotza, Dachamir . II.  
Manzato, Lizandro. III. Universidade Federal de Santa  
Catarina. Programa de Pós-Graduação em Engenharia Química.  
IV. Título.

Rodrigo Botinelly Nogueira

Green synthesis of silver nanoparticles  
using extract of seed skins of guaraná (*Paullinia cupana*)

*Síntese verde de nanopartículas de prata  
utilizando extrato de casquilhos de guaraná (Paullinia cupana)*

*A presente dissertação de mestrado será apresentada perante a banca examinadora  
composta pelos seguintes membros:*

Alexsandra Valerio, Dr.

Membro Externo/TNS

Prof. Débora de Oliveira, Dr.

Membro Interno/PósENQ-UFSC

*Certificamos que esta é a **versão original e final** do trabalho de conclusão que  
apresentada para obtenção do título de mestre em Engenharia Química.*

---

Prof. Débora de Oliveira, Dr.

Coordenadora/PósENQ-UFSC

---

Prof. Dachamir Hotza, Dr.

Orientador/PósENQ-UFSC

Prof. Lizandro Manzato, Dr.

Coorientador/IFAM

Florianópolis, 25/02/2022

Dedicated to my Parents, Marcio and Lígia,  
Also to my brother Rogério, my sister-and-low Yasmim, and my  
dogs Anne and Mr. Wesley.

## ACKNOWLEDGMENTS

My first thanks go to God, who has always been there for me for all eternity.

To Prof. Dachamir Hotza and Prof, Lizandro Manzato, for agreeing to be my advisors, not only for supporting me in good and bad moments but also for their teachings, guidance, understanding, and encouragement. You are my inspiration in my professional career.

To my parents Marcio Rogério Nogueira de Lima, Lígia de Jesus Botinelly, my brother, Rogério Botinelly Nogueira and my sister-in-law, Yasmim Botinelly. I am the result of the good education they gave to me. You are everything to me.

To the members of the examining board, for the willingness, for the time spent in evaluating this work, and for the dedication to contribute to the improvement of this thesis.

To all professors of the Graduate Program in Chemical Engineering (PósENQ) of the Federal University of Santa Catarina (UFSC), who always have demonstrated their best commitment and excellent education and scientific research.

To SisNANO network, despite the Covid-19 pandemic scenario, for the opportunity to work in different places such as the Federal Institute of Amazonas (IFAM), the State University of Amazonas (UEA), and their many laboratories:

- CMABio (UEA): Jander and Jessica, for TEM/SEM images
- LSCN (IFAM): Willian, who helped with questions and analysis
- LINDEN (UFSC): Emanoelle, for DLS measurements
- Applied microbiology laboratory: Rayane, for antibacterial activity analysis

To the Coordination for the Improvement of Higher Education Personnel (CAPES) for financial support.

To my friends, Amanda, Anézio, Caíque, Douglas, Érica, Igor, Ingridy, Jéssica, Juliana, Marcella, Marcus, Maria Tereza, Mateus, Noriane, Robson, Xavier, and Wanison for their fun moments and collaboration that made this journey healthier.

Finally, I would like to thank everyone who somehow supported me and contributed during this journey of academic formation.

*Have I not commanded you? Be strong and courageous. Do not be afraid, do not be discouraged, for the Lord your God will be with you wherever you go.*

(Joshua 1:9)

## RESUMO

Nanopartículas de prata (AgNPs) têm recebido grande atenção em virtude de suas propriedades únicas com aplicações em cosméticos, medicamentos, tratamento de água, entre outros. Tradicionalmente, nanopartículas metálicas podem ser sintetizadas usando reagentes tóxicos e perigosos por processos altamente energéticos. Como alternativa, a síntese verde mediada por extrato de plantas é eficiente, sustentável e barata. Nesse contexto, este trabalho tem como objetivo otimizar a síntese verde de AgNPs utilizando o extrato da pele da semente (casquilho) do guaraná (*Paullinia Cupana*) e avaliar sua atividade antibacteriana. Um planejamento experimental de Taguchi foi utilizado com propósito de otimizar a síntese e estimar a variabilidade da variável-resposta em termos dos parâmetros controláveis como também dos ruídos do processo. Nove experimentos (L9) foram realizados sendo avaliados três níveis de 4 propriedades (fatores controláveis): temperatura de reação, pH, concentração de AgNO<sub>3</sub> e concentração do extrato do casquilho do guaraná. O tamanho médio das AgNPs foi escolhida como variável-resposta. O extrato do casquilho do guaraná foi caracterizado pelo espectrômetro de massas por ionização por electrospray por ionização direta (DI-ESI-MS) e pela técnica de espectroscopia de fluorescência de raio (FRX). As AgNPs foram caracterizadas por técnicas de Espectroscopia Ultravioleta-Visível (UV-Vis), Infravermelho com Transformada de Fourier (FTIR), Difração de Raios-X (DRX), além de Espalhamento Dinâmico de Luz (DLS), Microscopia Eletrônica de Transmissão (MET), Microscopia Eletrônica de Varredura (MEV) e Espectroscopia de Emissão Atômica por Plasma Acoplado Indutivamente (ICP-OES). A atividade antibacteriana foi avaliada pela técnica de difusão em ágar contra *Staphylococcus aureus* e *Escherichia coli* e pela técnica de microdiluição em caldo para determinar a concentração inibitória mínima (CIM). A partir dos experimentos baseado em Taguchi, as AgNPs foram produzidas em condições otimizadas a pH = 11, concentração de AgNO<sub>3</sub> = 5 mM, temperatura de reação = 50°C, concentração do extrato do casquilho do guaraná = 1% (m/v). Nessas condições, foram obtidos menores tamanhos de AgNPs (26.11 nm com zeta potencial de -11.2 mV), como também uma menor variabilidade em termos de razão sinal/ruído (S/N). Pela técnica DI-ESI-MS, o extrato do casquilho do guaraná apresentou a cafeína como um dos possíveis compostos majoritário com subprodutos, como também, óxido de potássio como maior composição como apontado pelo FRX. Além disso, foi possível confirmar a presença de polifenóis, alcaloides, flavonoides e de compostos aromáticos, apontados como possíveis agentes redutores/estabilizadores. As AgNPs monodispersas com um formato quase-esférico foram observadas com a presença do extrato do casquilho do guaraná ao redor das partículas. Um alta concentração de nanopartículas de prata in a concentration of 180 ± 0.15 ppm foi detectado pela técnica da ICP-OES. Pela técnica da difusão em ágar, *E.coli* (15.7 ± 0.4 mm) demonstrou menor resistência sendo avaliados pelo halo de inibição quando comparados com a *S. aureus* (13.3 ± 0.2 mm) e obtendo os mesmos valores de CIM (50 µg/mL). Finalmente, a síntese verde apresentou robustez e eficácia, como também mostrou ser uma alternativa sustentável frente aos métodos tradicionais.

**Palavras-chave:** Síntese Verde; *Paullinia cupana*; Design experimental de Taguchi; Nanopartículas de prata; atividade antibacteriana.



## RESUMO EXPANDIDO

### Introdução

A palavra “nano” foi derivado do grego que significa pequeno. Na nanotecnologia, a nanoescala indica  $10^{-9}$  m ou um bilionésimo de metro. As nanopartículas de prata (AgNPs) vêm se destacando devido às suas propriedades únicas sendo aplicadas em medicamentos, catálise, tratamento de água, sensores, entre outros.

Tradicionalmente, as nanopartículas metálicas podem ser sintetizadas usando reagentes tóxicos e nocivos por processos de alta energia. Como alternativa, o método biológico por síntese verde de AgNPs usando extratos vegetais é não-tóxico, eficiente e sustentável. Portanto, cientistas têm se concentrado na síntese verde de nanopartículas de prata usando ferramentas estatísticas para promover uma maior robustez. O *Taguchi Design* pode ser aplicado quando há ruídos que podem influenciar as propriedades de um produto final.

Neste trabalho, emprega-se o casquilho do guaraná (*Paullinia Cupana*), um resíduo de Maués (Amazonas) que pode ser utilizado como potencial fonte de agentes estabilizantes/redutores. Além disso, as cascas das sementes de guaraná são utilizadas tradicionalmente como xarope sem valor comercial.

Portanto, neste trabalho apresenta-se a otimização da síntese verde de nanopartículas de prata utilizando cascas de sementes de guaraná como fonte de agentes estabilizantes/redutores. As nanopartículas de prata biossintetizadas são caracterizadas e avaliadas quanto à atividade antibacteriana.

### Objetivo

O principal objetivo deste trabalho foi a otimização da síntese verde de nanopartículas de prata via planejamento experimental de Taguchi avaliando sua eficácia na atividade antibacteriana. Esperou-se alcançar uma condição de maior robustez sendo alcançado um tamanho de nanopartícula de prata mínimo. Dessa maneira, decidiu-se variar os parâmetros que influenciam no tamanho das nanopartículas de prata (pH, temperatura, concentração do extrato do casquilho do guaraná e concentração de nitrato de prata). Com a condição otimizada, seu potencial bactericida foi avaliado.

### Metodologia

As matérias-primas utilizadas na síntese das nanopartículas de prata foram o extrato do casquilho do guaraná e o nitrato de prata. Para a síntese verde de nanopartícula de prata foi utilizada uma chapa aquecedora com agitação (IKA, C-MAG HS 10) sendo condicionada mediante as nove combinações estabelecidas pelo planejamento factorial de Taguchi avaliando

fatores dependentes (temperatura, pH, concentração de nitrato de prata e concentração do vegetal) e o tamanho médio das nanopartículas de prata como variável resposta. O casquilho do guaraná foi caracterizado utilizando DI-ESI-MS(LCQ fleet) e FRX (PW 2400). Na condição otimizada, amostras das AgNPs foram caracterizadas por UV-Vis (UV-1800), DRX (D2 Phaser), FT-IR (Cary 630), FRX(PW 2400), DLS (Zeta/Nanosizer), MET (1400 Flash), MEV (JSM IT500HR) e ICP-OES (ICPE-9820). A atividade antibacteriana foi avaliada pela técnica de difusão em ágar com cepas gram-positiva e gram-negativa, *Staphylococcus aureus* e *Escherichia coli*, respectivamente. A mensuração da concentração inibitória mínima foi determinada pela técnica da microdiluição em caldo.

### **Resultados e discussão**

O projeto experimental fatorial de Taguchi apontou a condição otimizada ( $C_{AgNO_3}$  de 5 mM,  $C_g$  de 1%, temperatura de 50°C, pH de 11), apresentando níveis com maior robustez. A composição do casquilho do guaraná apontou a cafeína como composto majoritário, além de outros ions na matriz vegetal. Por FRX, a análise dos elementos químicos envolvendo óxidos de cálcio, óxido de potássio e dióxido de silício apresentou elementos associados com a composição do casquilho do guaraná em pó. Por UV-Vis, compostos associados ao sistema anel benzoíla A foram detectados no extrato do casquilho do guaraná. Também foi observada a presença das AgNPs em evolução por um período de 30 dias, a influência do tamanho com o tempo, como também de sua polidispersão. Por DRX, os picos encontrados ((111), (200), (220), (311)) são referentes à prata (JCPDS 064706), sendo possível detectar a presença de sílica ( $SiO_2$ ) na matriz vegetal do casquilho do guaraná. Por FT-IR, grupos pertencentes a compostos alcoólicos e fenólicos foram detectados, assim como hidrocarbonetos em regiões mais baixas de número de onda. Os mesmos compostos, porém com menor intensidade, foram encontrados nas amostras de AgNPs que podem promover redução/estabilidade. O tamanho hidrodinâmico das AgNPs selecionadas foi de ~63.9 nm com zeta potential de -11.2 mV, ou seja, carga elétrica negativa. Por MET e MEV, foi possível verificar o formato quasi-esférico das AgNPs como também a presença do extrato do casquilho do guaraná ao redor das AgNPs. Valores de tamanho de partícula obtidos por DLS foram superiores aos encontrados por MET, o que se justifica pela natureza da técnica de mensuração. A solução otimizada de AgNPs apresentou valor de concentração de  $180 \pm 0.15$  ppm. O mecanismo de reação apresentou a cafeína como possível molécula capaz de reduzir e estabilizar as AgNPs. Pela atividade antibacteriana realizada pela técnica de agar em poços, as gram-negativas (*E.Coli*) apresentaram menor resistência quando comparadas com as gram-positivas (*S. Aureus*), possuindo halos de inibição de  $15.7 \pm 0.4$  mm e  $13.3 \pm 0.2$  mm, respectivamente. O extrato do casquilho do guaraná não apresentou halos de

inibição e a Levofloxacin (250  $\mu\text{g}/\text{mL}$ ) apresentou halo de inibição superior aos da AgNPs sendo de  $37.0 \pm 0.6$  mm e  $39.6 \pm 0.4$  mm, para *E.Coli* e *S. Aureus*, respectivamente. A concentração inibitória mínima para *E.Coli* e *S. Aureus* correspondeu à mesma concentração de 50  $\mu\text{g}/\text{mL}$ .

### **Considerações Finais**

As nanopartículas de prata foram sintetizadas a partir de método verde e caracterizadas pela amostra otimizada através do planejamento fatorial de Taguchi. As caracterizações do casquilho do guarana apontaram a cafeína como composto majoritário. Por FRX,  $\text{SiO}_2$  foi detectado, e confirmado pelo difratograma de DRX das AgNPs. UV-Vis apontou a presença de AgNPs, sendo possível mensurar o tamanho, polidispersão e observar o formato através das técnicas de microscopia (MEV e MET). Finalmente, foi possível encontrar uma concentração adequada de AgNPs. O mecanismo de reação da cafeína com a prata elucidou que é possível a utilização do extrato do casquilho do guaraná com nitrato de prata. Por fim, as AgNPs foram eficazes contra *S. aureus* e *E. coli*. Halos de inibição foram maiores no caso de gram-negativas, com a concentração inibitória mínima de 50  $\mu\text{g}/\text{mL}$ . Assim, este trabalho apresentou uma proposta de otimização via síntese verde de nanopartículas de prata, que foram aplicadas com sucesso em diferentes cepas bacterianas.

## ABSTRACT

Silver nanoparticles (AgNPs) have been standing out due to their unique properties being applied in cosmetics, medicines, water treatment, among others. Traditionally, metallic nanoparticles can be synthesized using toxic and harmful reactants by high-energy processes. As an alternative, green synthesis mediated by plant extracts is efficient, sustainable, and cheap. In this context, this work aims to optimize the green synthesis of AgNPs using the extract of the seed skin of guaraná (*Paullinia Cupana*) extracts and to evaluate their antibacterial activity. Taguchi experimental design was used to optimize the synthesis and to estimate the variability of the system response in terms of controllable parameters and noises in the process. Nine experiments (L9) were carried out at three levels of 4 properties (controlled factors): reaction temperature, pH, AgNO<sub>3</sub> concentration, and guaraná seed skin extract concentration. The average size of AgNPs was chosen as the response variable. The guaraná seed skin extract was characterized by the direct infusion electrospray ionization mass spectrometer (DI-ESI-MS) and by the ray fluorescence spectroscopy (XRF) technique. AgNPs were characterized by spectroscopy techniques, such as Ultraviolet-Visible spectroscopy (UV-Vis), Fourier-Transform Infrared Spectroscopy (FTIR), X-Ray Diffraction (XRD), as well as Dynamic Light Scattering (DLS), Transmission Electron Microscopy (TEM), Scanning Electron microscopy (SEM) and Inductively coupled plasma atomic emission spectroscopy (ICP-OES). Antibacterial activity was evaluated using well-agar diffusion against *Staphylococcus aureus* and *Escherichia coli* by the broth microdilution method to determine the minimum inhibitory concentration (MIC). From Taguchi experiments, the AgNPs were produced the optimized conditions at pH = 11, AgNO<sub>3</sub> concentration = 5 mM, reaction temperature = 50 °C and concentration of guaraná seed skin = 1% (m/v). At those conditions, AgNPs were obtained with the smallest size (26.11 nm and zeta potential of -11.2 mV), as well as with less variability in terms of signal-to-noise ratio (S/N). By the DI-ESI-MS technique, the guaraná seed skin extract showed caffeine as one of the possible major compounds with by-products, as well as potassium oxide as the highest composition as pointed out by the XRF. In addition, the presence of polyphenols, alkaloids, flavonoids, and aromatic compounds was detected as possible reducing or/and stabilizing agents. Monodisperse, quasi-spherical AgNPs were observed with the presence of guaraná seed skin extract around the particles. A high concentration of silver nanoparticles of 180 ± 0.15 ppm was detected using ICP-OES. In the well-agar diffusion method, *E.coli* (15.7 ± 0.4 mm) demonstrated lower resistance being evaluated by the zone of inhibition when compared with *S. aureus* (13.3 ± 0.2 mm) and achieved the same value of CIM (50 µg/mL). Finally, the green synthesis presented robustness and efficiency and it was shown to be a sustainable alternative to the traditional methods.

**Keywords:** Green synthesis; *Paullinia cupana*; Taguchi experimental design; silver nanoparticles; antibacterial activity.

## LIST OF FIGURES

Figure 1 - <i>Paullinia cupana</i> (guaraná): (A) Orange fruits with red capsules containing black seeds partially covered by white aril. (B) Collected seeds partially covered by arils, and dried powdered seeds.....	24
Figure 2 - Guaraná roasting in Maués region, Amazonas, Brazil. ....	25
Figure 3 - Municipalities where guaraná is produced in Amazonas, Brazil.....	26
Figure 4 - Nanomaterials classification according to their dimensions. ....	29
Figure 5 - Synthesis of nanomaterials according to the top-down and bottom-up approaches. ....	30
Figure 6 - Mechanisms of stabilization of nanoparticles.....	31
Figure 7 - Hypothetical mechanism of action of silver nanoparticles in bacteria. ....	32
Figure 8 - Structure of gram-negative and gram-positive bacteria.....	33
Figure 9 - Taguchi method used for the optimization of synthesis parameters.....	40
Figure 10 - Broth microdilution method using 96 well-plates.....	46
Figure 11 - Influence of single factors on the average size of AgNPs and respective signal-to-noise ratio (S/N): concentration of silver nitrate ( $C_{AgNO_3}$ ), the temperature of the reaction, the concentration of guaraná seeds skins extract ( $C_g$ ), and pH.....	48
Figure 12 - Pareto chart of the standardized effects (Response in size (nm) $\alpha = 0,1$ ).....	50
Figure 13 - Response surfaces in relation to the average size of AgNPs: concentration of silver nitrate ( $C_{AgNO_3}$ ), temperature of reaction, concentration of guaraná seed skins extract ( $C_g$ ), and pH.....	51
Figure 14 - DI- ESI-MS fingerprints of guaraná seed skins extract in positive mode in 100-600 m/z.....	52
Figure 15 - Products ions spectra of fragmentation of caffeine in peak at m/z 195.....	53
Figure 16 - Absorption spectra of AgNPs observed in 1h, 24 h, and 30 days of reaction.....	53
Figure 17 - AgNPs SPR peak intensity.....	57
Figure 18 - Color change AgNPs (1 h, 24 h, and 30 days).....	57
Figure 19 - XRD spectrum of AgNPs.....	58
Figure 20 - FTIR spectra of the guaraná seeds skin extract and the as-prepared AgNPs.....	59
Figure 21 - Zeta potential and particle size distribution of AgNPs derived from seed skin guaraná extract.....	61
Figure 22 - SEM micrographs of AgNPs obtained by green synthesis using <i>Paullinia Cupana</i> extract at different magnifications: (a) 5,000 $\times$ , (b) 20,000 $\times$ , (c) 100,000 $\times$ and (d) 200,000 $\times$ ...	62

Figure 23 - TEM micrographs of AgNPs obtained by green synthesis using <i>Paullinia Cupana</i> extract. a) AgNPs micrograph at 200 nm. b) Presence of seed skins Guaraná, extract c) Histogram of AgNPs.....	63
Figure 24 - Suggested mechanism for the silver ion to mellatic silver nanoparticles via caffeine as reducing agent.....	65
Figure 25 - Stabilization of silver nanoparticles performed by caffeine molecule present in the guaraná seed skins extract.....	65
Figure 26 - Antibacterial activity of biosynthesized AgNPs using guaraná seed skins extract against <i>E. Coli</i> and <i>S.Aureus</i> .....	67
Figure 27 - Determination of minimum inhibitory concentration (MIC) of AgNPs after 24h against <i>S. aureus</i> and <i>E. coli</i> .....	69

## LIST OF TABLES

Table 1. Chemical compounds identified in guaraná seeds extract.....	27
Table 2. Selected green synthesis of silver nanoparticles using plant extracts.....	34
Table 3. AgNPs synthesis parameters (factors) and their levels. ....	40
Table 4. Taguchi's L9 orthogonal array.....	41
Table 5. Equipment used in the synthesis and characterization of AgNPs.....	43
Table 6. Optimization of parameters in the synthesis of AgNPs.....	47
Table 7. Analysis of variance (ANOVA) of the regression equation of size of AgNPs.....	50
Table 8. Chemical analysis of oxides elements of guaraná seed skin by X-ray fluorescence .....	54
Table 9. Bands in the FTIR spectra of guaraná seed skin extract and as-prepared AgNPs.....	60
Table 10. Inhibition zone (mm) of AgNPs using agar well diffusion method.....	68

## LIST OF ABBREVIATIONS AND ACRONYMS

AgNPs	Silver Nanoparticles
AMBEV	America's Beverage Company
ANOVA	Analysis of Variance
BOD	Biochemical Oxygen Demand
CCCD	Cefar diagnostic culture collection
CLSI	Clinical Laboratory Standards Institute
CMaBio	Multiuser Center for the Analyses of Biomedical Phenomena
DLS	Dynamic Light Scattering
EMBRAPA	Brazilian Agricultural Research Corporation
ESI-MS	Electrospray Ionization Mass Spectroscopy
FTIR	Fourier-Transform Infrared spectroscopy
GAE	Gallic Acid Equivalent
ICP-OES	Inductively Coupled Plasma Atomic Emission Spectroscopy
JCPDS	Joint Committee on Powder Diffraction Standards
LABCEM	Laboratory of Chromatography and Mass Spectrometry
LINDEN	Interdisciplinary Laboratory for the Development of Nanostructures
LSCN	Laboratory of Synthesis and Characterization of Nanomaterials
MIC	Minimum Inhibitory Concentration
NM	Nanomaterial
ROS	Reactive Oxygen Species
SEM	Scanning Electron Microscopy



SPR	Surface Plasmon Resonance
S/N	Signal-to-Noise ratio
TEM	Transmission Electron Microscopy
UFAM	Federal University of Amazonas
UFSC	Federal University of Santa Catarina
USFDA	US Food and Drug Administration
UV-Vis	Ultraviolet-Visible spectroscopy
XRD	X-ray Diffraction
XRF	X-Ray Fluorescence

## LIST OF SYMBOLS

<i>CAgNO3</i>	Silver Nitrate Concentration	[mM]
<i>Cg</i>	Guaraná Seed Skins concentration	[% mass/volume]
<i>m/z</i>	Mass-to-charge	dimensionless
<i>MIC</i>	Minimum Inhibitory Concentration	[mg/mL]
<i>pH</i>	Potential of Hydrogen	[-]
<i>T</i>	Temperature	[°C]
<i>ZOI</i>	Zone of Inhibition	[mm]

## SUMMARY

<b>1</b>	<b>INTRODUCTION AND GOALS.....</b>	<b>21</b>
1.1	MAIN GOAL.....	23
1.2	SPECIFIC GOALS.....	23
<b>2</b>	<b>THEORETICAL BACKGROUND.....</b>	<b>24</b>
2.1	GUARANÁ: PLANT AND PRODUCTS.....	24
2.2	CHEMICAL COMPOSITION.....	26
2.3	NANOTECHNOLOGY AND NANOMATERIALS.....	28
2.4	SILVER NANOPARTICLES: CHARACTERISTICS AND SYNTHESIS.....	31
2.5	GREEN SYNTHESIS USING EXTRACTS DERIVED FROM PLANTS.....	333
<b>3</b>	<b>MATERIALS AND METHODS.....</b>	<b>39</b>
3.1	OPTIMIZATION OF SYNTHESIS PARAMETERS.....	39
3.2	PROCESSING METHODS.....	41
3.3	CHARACTERIZATION METHODS.....	42
3.3.1	X-Ray Fluorescence (XRF) .....	43
3.3.2	Inductively coupled plasma atomic emission spectroscopy (ICP-OES) .....	43
3.3.3	Ultraviolet-visible-spectroscopy (UV-Vis).....	44
3.3.4	Dynamic Light Scattering (DLS).....	44
3.3.5	Fourier-Transform Infrared Spectroscopy (FTIR).....	44
3.3.6	X-Ray Diffraction (XRD) .....	44
3.3.7	Scanning Electron Microscopy (SEM) and Transmission Electron Microscopy (TEM).....	45

3.4 ANTIBACTERIAL ACTIVITY EVALUATION.....	45
<b>4 RESULTS AND DISCUSSIONS.....</b>	<b>47</b>
4.1 OPTIMIZATION OF SILVER NANOPARTICLES SYNTHESIS.....	47
4.2 CHARACTERIZATION OF SELECTED SILVER NANOPARTICLES.....	52
<b>4.2.1 Chemical profile of extract by Direct Infusion Electrospray ionization mass spectrometry (DI-ESI-MS) .....</b>	<b>52</b>
<b>4.2.2 X-ray fluorescence (XRF) of seed skins of guaraná (<i>Paullinia cupana</i>) .....</b>	<b>54</b>
4.3 CHARACTERIZATION OF SELECTED SILVER NANOPARTICLES.....	56
<b>4.3.1 UV-Vis Spectroscopy.....</b>	<b>56</b>
<b>4.3.2 X-ray Diffraction (XRD).....</b>	<b>58</b>
<b>4.3.3 Fourier-Transform Infrared Spectroscopy (FTIR).....</b>	<b>59</b>
<b>4.3.4 Particle size distribution and zeta potential .....</b>	<b>61</b>
<b>4.3.5 Microscopy analysis (SEM and TEM).....</b>	<b>62</b>
<b>4.3.6 Inductively coupled plasma atomic emission spectroscopy (ICP-OES).....</b>	<b>64</b>
4.4 PROPOSED MECHANISM OF THE FORMATION OF SILVER NANOPARTICLES.....	65
4.5 ANTIBACTERIAL ACTIVITY OF SILVER NANOPARTICLES .....	67
<b>5 CONCLUSIONS AND PERSPECTIVES.....</b>	<b>70</b>
<b>REFERENCES.....</b>	<b>72</b>

## 1. INTRODUCTION AND GOALS

In 1959, in a lecture entitled “*There is plenty of room at the bottom*” to a meeting of the American Physical Society, Richard Feynman highlighted the possibilities of work on a small scale and discussed how nanotechnology can provide answers to many fundamental questions. Indeed, his speech outlined a vision of nanotechnology that revolutionized modern science as a multidisciplinary field, combining chemistry, physics, biology, medicine, and other subjects (RAFIQUE, 2020).

Although the concept of nanotechnology is considered a new science, the manipulation of nanomaterials has been in use for centuries. The classic evidence of the use of nanomaterial in human history is the Lycurgus cup which changes colors depending on the location of the light source. It looks green in reflected light and red when it shines through it due to the colloidal dispersion by gold and silver nanoparticles (LEON, 2020).

According to US Food and Drug Administration (USFDA), every object possessing at least one dimension between 1 and 100 nm can be classified as a nanomaterial (GUIDANCE, 2011). When dealing with a high surface area to volume ratio, the novel optical, mechanical, electronic, and magnetic properties of nanomaterials (NMs) become remarkable and unique when compared to the bulk materials. Indeed, the global nanomaterial markets (nanotubes, nanoparticles, nanoclay, nanowires, among others) have grown from USD 4.7 billion in 2017 to USD 13 billion by 2021 (RAJ, 2022).

Among diverse metallic nanoparticles, silver nanoparticles (AgNPs) are one of the most promising nanomaterials (RAJ, 2022). AgNPs present remarkable and novel properties, such as suitable electric conductivity, chemical stability, and antimicrobial activity. (KAKAKHEL et al, 2021) In the last decades, AgNPs have gained significant attention by the industry being highly commercialized as several products (Nanodatabase, 2021). AgNPs are reported to have a wide range of use due to their physical, chemical, and biological properties with successful applications in biomedicine (BURDUSEL, A. 2018), drug-delivery formulations (JAHANGIRIAN, 2017), treatment of cancer (VLÂSCEANU, 2016), catalysis (SHAKER, 2021), water purification (QUE, 2018), antimicrobial activity (SOFI, M. et al, 2021), among others.

AgNPs can be synthesized following three main paths: physical, chemical, and biological approaches. In the physical method, no hazardous reagents are involved, but high energy demand is required increasing the cost of operation (ZHANG, X et al, 2016). In the

chemical methods, hydrazine, sodium borohydride, and polyethylene glycol (PEG) are commonly used as reducing agents while polyvinylpyrrolidone (PVP) is used as a stabilizing agent (MONTAZER, 2012). These substances are toxic and harmful to living organisms and the environment. As an alternative, biological methods are considered ecofriendly and low-cost since the raw materials are obtained from the environment. (RAUWEL, 2015)

In recent years, plant extracts have received huge consideration as sustainable sources of reducing and stabilizing agents. In green synthesis approaches, the use of plants extracts, aminoacids, proteins, polysaccharides, alkaloids, and vitamins can enhance the production of stabilized silver nanoparticles (SIDDIQI, 2018). Diverse substances can be extracted from plants; the purity and concentration depend on the area where the crops are cultivated, the water/soil conditions, and the anatomic structure of the plants. (GRAÇA, 2015).

Brazil is recognized as a host of a huge number of plants and it is considered the most biologically diverse country in the world. In Amazonia, it is reported that just only a fraction of plants were cataloged and studied (TER STEEGE, 2016). Guaraná (*Paullinia cupana*), a native Amazonian plant, is found majorly in Brazil, with some occurrences in Venezuelan and Peruvian regions. Guaraná processing leaves bark residues, being the seed skin 20% of its weight, which is disposed to the environment without any application (MICHILES, 2010).

Silver has been used extensively because of its strong toxicity being effective in antimicrobial applications (ALEXANDER, 2009). However, the exact mechanism of interaction between AgNPs and microorganisms is still under debate. Nevertheless, the antimicrobial activity of AgNPs depends upon particle size, shape, and distribution. (RAZA, 2016). Moreover, temperature, reaction time, concentration of the metal precursor, concentration of reducing agents, and pH can influence the structure, morphology, and size of AgNPs (SHAIKH, 2021).

Several studies on green synthesis using plant extracts have been dedicated to elucidate the mechanism between the components from plant extract and silver ions or nanoparticles. To the best of our knowledge, there is no report about extracts from guaraná seeds or wastes applied to the synthesis of AgNPs yet. In this context, AgNPs were synthesized using guaraná seed skin extract as a source of reducing/stabilizing agents. The Taguchi Design was proposed as a statistical method to optimize the process and to analyze parameters that affect it. Subsequently, the selected AgNPs were characterized physically and chemically. Lastly, AgNPs were evaluated *in vitro* in terms of antibacterial activity in different biological systems.

## 1.1 MAIN GOAL

The main goal is to optimize the green synthesis of silver nanoparticles using guaraná seed skin extracts and to evaluate their antibacterial properties.

## 1.2 SPECIFIC GOALS

To achieve the main goal, the specific goals are:

- Selection of the synthesized AgNPs according to different process conditions such as pH, nitrate silver concentration, guaraná extract concentration, and temperature of reaction;
- Characterization of guaraná seed skins using DI-ESI-MS and XRF.
- Characterization of optimized AgNPs through chemical and physical methods such as UV-vis, FTIR, DLS, TEM, SEM, ICP-OES, and XRD;
- Study of stability of AgNPs suspensions in long term;
- Evaluation of the antibacterial activity *in vitro* of AgNPs against *Escherichia coli* and *Staphylococcus aureus*.

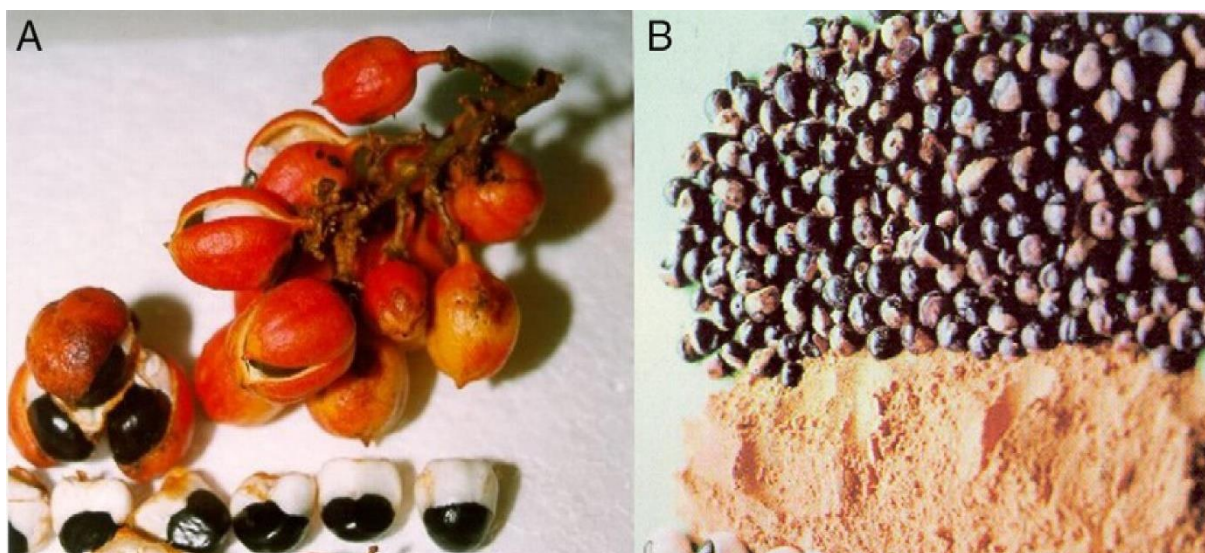
## 2. THEORETICAL BACKGROUND

In this Chapter, a detailed review was prepared to introduce critical aspects about the guaraná plant, nanotechnology, and nanoparticles, which are the main topics inherent to this work.

### 2.1 GUARANÁ: PLANT AND PRODUCTS

The guaraná (*Paullinia cupana*) is a Brazilian native plant of the family *Sapindaceae* (SELLAMI, 2018). The guaraná plant is a lowland, tropical, woody, climbing shrub, which is adapted to a hot and humid climate. The fruits are ellipsoidal or spherical, apiculate capsules that are red when ripe and measure 2–3 cm (Figure 1A). They have 1 or 2 egg-shaped seeds, of ~12 mm in length, with an abundant aril before maturity. Commonly, guaraná seeds are toasted and ground into powder (Figure 1B). Guaraná finds application mainly in the soft drinks industry, although it is also highly employed in cosmetic and pharmaceutical products. (MARQUES, 2019)

Figure 1 - *Paullinia cupana* (guaraná): (A) Orange fruits with red capsules containing black seeds partially covered by white aril. (B) Collected seeds partially covered by arils, and dried powdered seeds.



Source: MARQUES, 2019 (adapted).

The origin of guaraná is usually associated with the central and lower Amazon regions, between Madeira and Tapajós rivers. (DUCKE, 1937) Firstly, guaraná was domesticated and cultivated by the Sateré-Mawé tribe. (FIGUEROA, 2016), who spread. Maués is known as the “land of guaraná” since the time of the colonial conquest of the Amazon. (LORENZ, 1992)



Traditionally, guaraná crop is carried out by traditional agriculture methods. Firstly, the fruits are packed in bags for up to three days to start the fermentation process. In the cleaning process, the seeds are washed with water (usually in the riverside) and classified by sieving into size ranges (MICHILES, 2010). The seeds are then roasted in ceramic or metal ovens to achieve a minimum moisture level, and to obtain a more homogeneous product (Figure 2).

Figure 2 - Guaraná roasting in Maués region, Amazonas, Brazil.

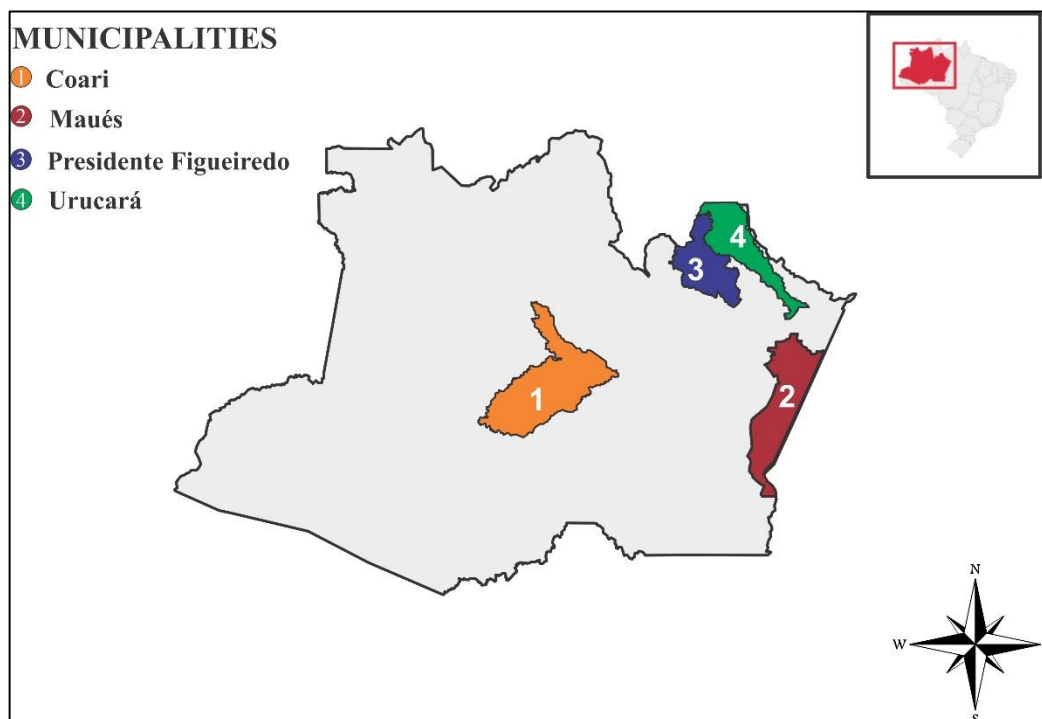


Source: <https://m.facebook.com/aliancaguaranádemaues>

After cooling, the seeds are stored in bags made of natural fibers for up to 18 months depending on the storage conditions. The skin is removed from the seeds using mechanized peeling equipment. Guaraná is widely used in the food industry in the form of syrups, extracts, and distillates, primarily as a flavoring agent and as a source of caffeine by soft drink manufacturers (LEDO, 1996; ANTUNES, 2011; SILVA, 2018).

According to Embrapa (2005), Brazil is practically the only producer in the world, with only small cultivated areas present in Venezuela and Peru. In Brazil, Amazonas, Bahia, and Mato Grosso represent ~93.5% of national production in 2018. The main producing state is Bahia with 60% of national production in 2018. In Amazonas, guaraná is cultivated in 15 municipalities. Maués, Presidente Figueiredo, Coarandi and Uruará are responsible for ~76% of the total state production in 2018 (Figure 3) (CONAB, 2019).

Figure 3 - Municipalities where guaraná is produced in Amazonas, Brazil



Source: GUIA GEOGRÁFICO, 2022 (Adapted)

AMBEV, a beverage company in Brazil, demands 70% of guaraná seeds produced in Maués region, and this market is expected to increase (SUFRAMA, 2003). However, the production of guaraná in Amazonas has been declining when compared to Bahia State (BOGAS, 2015). A limiting factor to the production and expansion of guaraná crops in Amazonas are diseases, such as anthracnose, which is caused by the fungus *Colletotrichum guaranicola* Albuq (SANTOS, 2021).

## 2.2 CHEMICAL COMPOSITION

Guaraná seeds are the commercially useful part of the plant because of the large amounts of caffeine, theobromine, and theophylline, as well as the high concentration of tannins and other compounds, such as saponins, polysaccharides, proteins, and fatty acids. (LORENZI, 2002). In a recent study, high contents of tannins, methylxanthines, and type-A-procyanidin trimer were identified in guaraná powdered seeds (MACHADO, 2021).

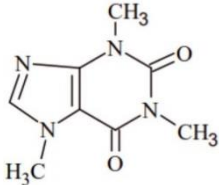
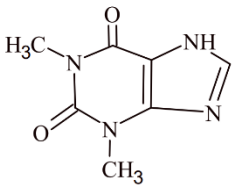
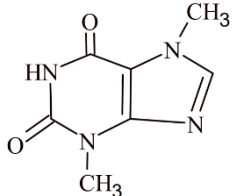
In addition, the phenolic content of guaraná seeds extract is influenced by which solvent is used according to its polarity. It is reported that using 35% acetone, the phenolic content is 186 mg GAE/g extract at 85 °C being more efficient than water, methanol, or other solvents

(MAJHENIC, 2007). Also, the extraction of phenolic content from the extract of guaraná seeds has been performed successfully by using water-ethanol mixtures (10-90%). The best condition of extraction of phenolic compounds was with a 50%/50% hydroalcoholic solution reaching a content of ~434 mgGAE/g (SILVA, 2019).

Capillary electrophoresis and liquid chromatography (HPLC) have been used to identify compounds such as caffeine, theobromine and theophylline were identified compounds present in the guaraná seeds extract. (SOMBRA, 2005). Furthermore, it was reported that a high concentration of caffeine (102.9 mg/g), followed by theophylline (2.3 mg/g) and theobromine (1.0 mg/g) (PEIXOTO, 2017). In another work, the same technique of characterization was reported in which epicatechin (146 mg/g) and catechin (98 mg/g) were identified as compounds present in the guaraná seeds extract (SILVA, 2019).

Extraction and solvent type can naturally influence the yield and efficiency of the process such that different contents of active compounds can be achieved (PINHO, 2021). In Table 1, some components identified in guaraná seeds extracts are presented according to the literature.

Table 1. Chemical compounds identified in guaraná seeds extract.

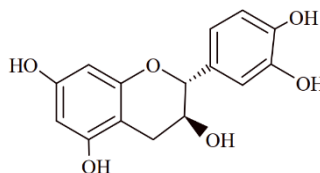
<b>Methylxanthines</b>		
<b>Popular/Chemical name</b>	<b>Chemical Structure</b>	<b>References</b>
Caffeine (1,3,7- Trimethylxanthine)		(PEIXOTO, 2017); (SOMBRA, 2005)
Theophylline (1,3-dimethylxanthine)		(PEIXOTO, 2017); (MARQUES, 2016)
Teobromine (3,7-dimethylxanthine)		(PEIXOTO, 2017); (DE MARIA, 2007)

---

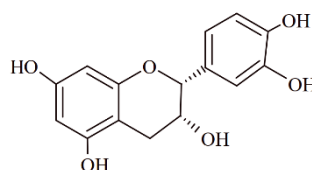
**Tanines**


---

(+) – Catechin


 (CARDOSO, 2002);  
 (VEGGI, 2013).

(-) - Epicatechin


 (CARDOSO, 2002);  
 (ANTUNES, 2011)

 Source : (Author, 2022)
 

---

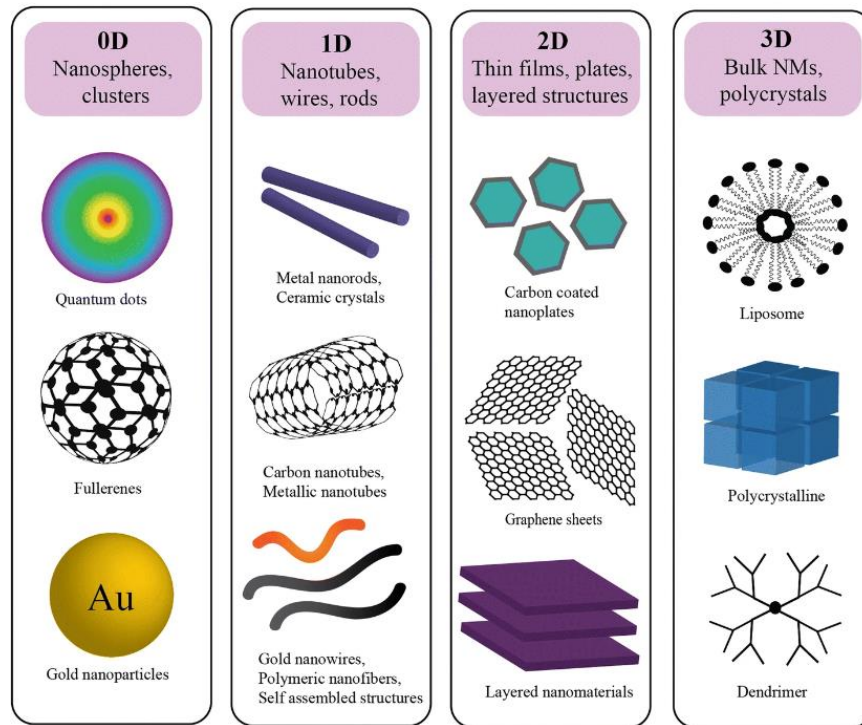
### 2.3 NANOTECHNOLOGY AND NANOMATERIALS

In 1959, at the annual conference of the American Society of Physics, Richard Feynman predicted that “There’s a lot of room at the bottom” as an invitation to explore nanotechnology. In 1974, the term “nanotechnology” was coined by Norio Taniguchi to relate the tolerable dimensions of the machining and finishing process for semiconductor materials (DOLEZ, 2015). The prefix “nano” is derived from the Greek meaning the billionth of a unit.

According to the 2011 European Commission report, the definition of nanomaterial is a material – natural, incidental, or manufactured – containing particles in which 50% or more of the particles in one or more dimensions are in the range of 1 to 100 nanometers. (EC, 2011)

Nanomaterials can be classified into four categories based on the criteria of their dimensionality, as shown in Figure 4 (POH, 2018).

Figure 4 - Nanomaterials classification according to their dimensions.



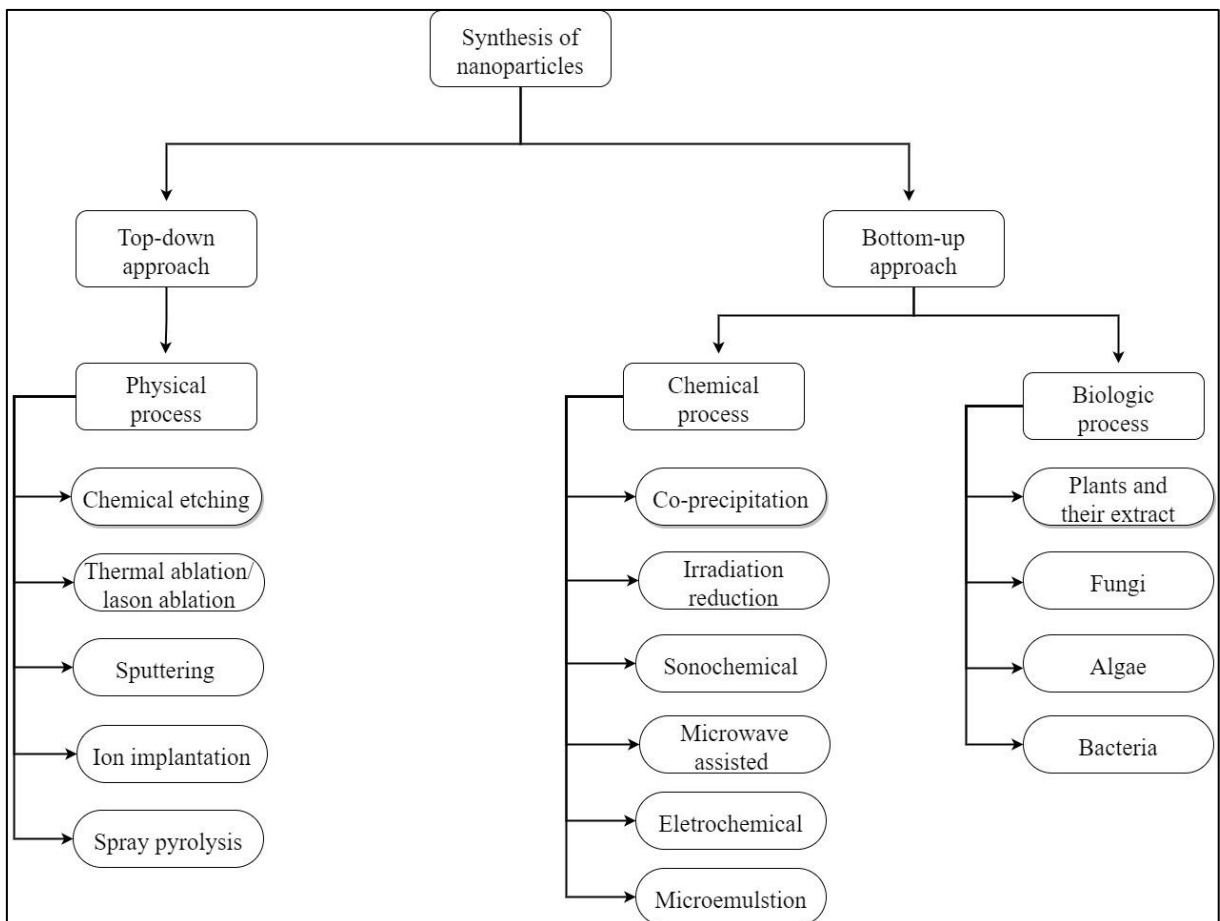
Source: POH, 2018 (Adapted)

For zero dimension nanomaterials (0D), all dimensions are nanometric scales. Examples of 0D nanomaterials are quantum dots, fullerenes, or metal nanoparticles, which are usually applied as sensors and catalysts. (PEIPEI, 2020). One dimension (1D) nanomaterials are those that have two outer dimensions at the nanoscale, while the outer dimension is usually found at the microscale. Examples of 1D nanomaterials include nanotubes, nanowires, and nanorods. Two-dimension (2D) nanomaterials contain only one nanoscale dimension, while the other two dimensions are on the microscale. Examples of 2D nanomaterials are thin films, nanoplates, nanocoatings, etc (DOLEZ, 2015). Three-dimension (3D) nanomaterials have various dimensions beyond 100 nm and combine multiple nanocrystals in different directions. Examples can be nanocomposites and nanostructured nanomaterials. (SALEH, 2020)

NPs can be found in different forms, such as quantum dots, fullerenes, nanorods, and nanoplates. In addition, they can be got in different shapes including spherical, triangular, hexagonal, and ellipsoidal. (RODRIGUES, 2021; NAIR, 2021)

Nanoparticles can be obtained following two main paths: bottom-up and top-down methods (Figure 5). The top-down approach uses techniques to break down the particles into a nanoscale, in other words, materials in bulks are reduced/fragmented to nanoscale materials in different techniques, such as thermal decomposition, laser ablation, mechanical milling, and etching. (SHARMA, 2021) In contrast, *bottom-up* approach, nanomaterials are formed by “self-assembly” that includes arrangements of smaller components into more complex structures which can be performed in some techniques, such as chemical reduction, spinning, sol-gel process, and green synthesis (RANA, 2020).

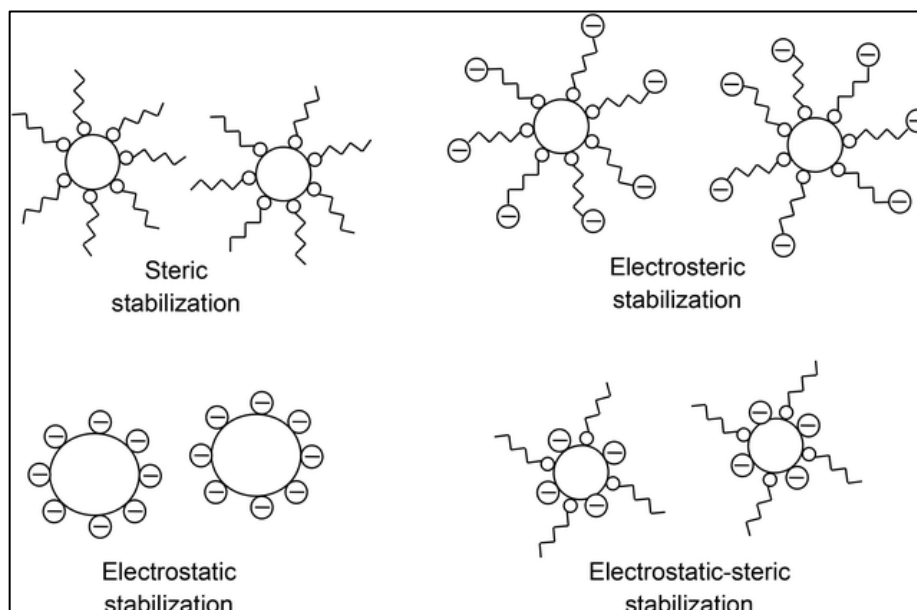
Figure 5 - Synthesis of nanomaterials according to the top-down and bottom-up approaches.



Source: OVAIS, 2017 (Adapted)

Nanoparticles exhibit a high area/volume ratio, which frequently causes agglomeration along the time as a strategy to minimize the superficial energy. When these particles are together, they are called aggregates. Three mechanisms of stabilization can be employed to avoid agglomeration: steric, electrostatic, or a combination of both, as shown in Figure 6.

Figure 6 - Mechanisms of stabilization of nanoparticles.



Source: TAN, 2016

Steric stabilization occurs when a molecular chain is attached to some point at the surface of the nanomaterial and there are mobile branches in solution. In the case of electrostatic stabilization, charges are located on the surface of the particles. Negative (or positive) charged particles repel other particles with the same charge. Those two basic mechanisms can be combined as electrosteric or electrostatic-steric stabilization, with the aid of respective surfactant molecules (TAN, 2016).

#### 2.4 SILVER NANOPARTICLES: CHARACTERISTICS AND SYNTHESIS

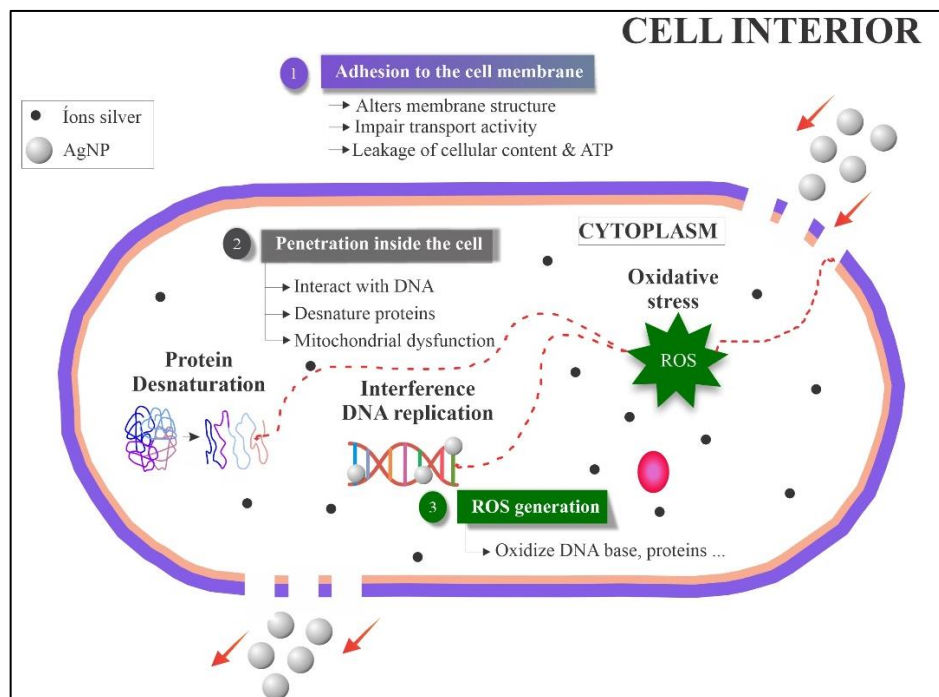
Among all metallic nanoparticles, silver nanoparticles have stood out due to their unique properties (MAHMOUD, 2021). Since ancient years, silver has exhibited toxicity for diverse types of microorganisms. In nano form, silver possesses a higher ratio of surface to volume when compared to bulk materials, which makes them more toxic. However, the exact mechanism of silver nanoparticles in bacteria is not fully understood yet (PAREEK et al, 2018). Moreover, it has gained much attention as a promising alternative to antibiotic therapy because silver nanoparticles (AgNPs) exhibit a huge potential for solving problems associated with the development of multidrug resistance against pathogenic microorganisms (AHMAD, 2020).

The efficiency of AgNPs as a biocide depends basically upon the shape, size, pH, and ionic strength of the medium. The AgNPs can act as a reservoir and they can continually release

silver ions ( $\text{Ag}^+$ ) which might be considered one potential mechanism of killing microbes (DAKAL, 2016). Moreover, AgNPs with a spherical or quasi-spherical format are more prone to release silver ions due to their larger surface area (YIN, 2020).

A mechanism for the antibacterial activity of AgNPs is proposed in Figure 7, and can be understood in some steps:

Figure 7 - Hypothetical mechanism of action of silver nanoparticles in bacteria.



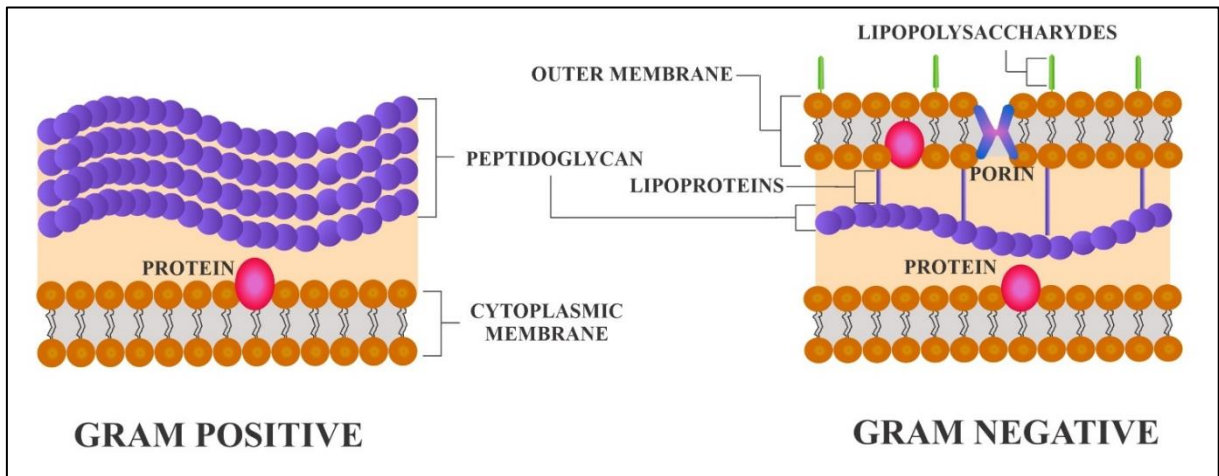
Source: AHMAD, 2020 (Adapted)

Firstly, silver nanoparticles exhibit affinity towards sulfur proteins due to the electrostatic attractions and they can adhere to the cell wall and cytoplasm membrane resulting in its disruption. Then, free silver ions ( $\text{Ag}^+$ ) are uptaken by the cells and they can also alter transport and the release of potassium ( $\text{K}^+$ ) affecting the transport activity and leading to the production of reactive oxygen species (ROS). Consequently, they can interrupt adenosine triphosphate (ATP) activity. (AHMAD, 2020)

Inside the bacterial cell, the action of AgNPs can be attributed to interaction with ribosomal components interrupting the protein synthesis. The antimicrobial potential of AgNPs can interact with gram-negative or gram-positive bacteria, as shown in Figure 8 (DUVAL, 2019).



Figure 8 - Structure of gram-negative and gram-positive bacteria.



Source: SLAVIN, 2017 (Adapted).

Some studies suggest that gram-negative bacteria are more susceptible than gram-positive bacteria when exposed to AgNPs. The peptidoglycan of gram-positive bacteria is thicker than those in gram-negative bacteria, which prevents to some extent the action of AgNPs. In fact, smaller AgNPs are more susceptible to penetrate bacteria resulting in higher toxicity (YIN, 2020).

## 2.5 GREEN SYNTHESIS USING EXTRACTS DERIVED FROM PLANTS

The use of plant extracts as a source of biomolecules responsible for the synthesis of silver nanoparticles has been explored increasingly in the last few years. Table 2 shows a selection of diverse plant extracts, which are the precursor for the green synthesis of AgNPs. To the best of our knowledge, extracts from guaraná have not yet been used for this purpose.

Table 2. Selected green synthesis of silver nanoparticles using plant extracts.

<b>Plant extracts</b>	<b>Biomolecules</b>	<b>Shape</b>	<b>Nanoparticle Size (nm)</b>	<b>Reference</b>
<i>Aerva lanata</i>	Proteins, polyphenols, flavonoids, alkaloids, saponins.	Spherical	2-10	PALITHYA, 2021
<i>Aloe vera</i>	N/A	Spherical	30-50	SINGH, 2021
<i>Aloe vera</i>	Polysaccharides, uronic acid	N/A	N/A	ANJU, 2021
<i>Ammania bacifera</i>	N/A	Hexagonal, triangular, Spherical, rod.	112	JADHAV, 2016
<i>Artocarpus heterophyllous;</i> <i>Azadirachta indica</i>	Polyphenols, phenolic compounds, carbonyl compounds, flavonoids, and alkaloids	Spherical	20-40	MANIK, 2020
<i>Asparagus officinalis</i>	Phenolic compounds, flavonoids, proteins	Spherical	16	TRIPATHI, 2021
<i>Azadirachta indica.</i>	Proteins, flavonoids, and terpenoids	Spherical	10-63	BALACHANDRAN, 2012
<i>Biophytum sensitivum</i>	N/A	Spherical	8	KAVITHA, 2021

<i>Borago officinalis</i>	Flavonoids, polysaccharides, proteins	Irregular spherical and hexagonal	30-80	SINGH, 2017
<i>Brosimum gaudichaudii</i>	Phenolic compounds	Spherical	21	SILVA, 2014
<i>Carthamus tinctorius L.</i>	Proteins, polysaccharides, phenolic compounds, flavonoids	Spherical	2-50	RODRÍGUEZ-FÉLIX, 2021
<i>Celastrus paniculatus</i>	Flavonoids and phenolic compounds	Spherical	2-10	MALI, 2020
<i>Ceropegia thwaitesii</i>	Polysaccharides, proteins	Spherical	100	MUTHUKRISHNAN, 2015
<i>Chenopodium album</i>	N/A	Spherical	N/A	ANANDALAKSHMI, 2021
<i>Cinnamomum camphora</i>	Proteins, saturated alcohol	Spherical	19	LI, 2021
<i>Citrus aurantifolia</i>	N/A	Almost Spherical	80-120	CHOWDHURY, 2021
<i>Citrus limetta</i>	Alcoholic compounds	Spherical	18	DUTTA, 2020
<i>Cleome viscosa L.</i>	Alkaloids, phenolic compounds, tannis	Spherical	5-30	LAKSHMANAN, 2018
<i>Coriander sativum</i>	Flavonoids, phenolic compounds	Spherical	67-86	ALSUBKI, 2021
<i>Cymbopogon citratus</i>	Flavonoids, polyphenols	Irregular cubic	9	PATINO-RUIZ, 2020

<i>Elaeagnus angustifolia</i>	Flavonoids	Spherical	65-90	MORTAZAVI- DERAZKOLA, 2021
<i>Emblica officinalis</i>	Alkaloids, phenolic compounds, tannis	Spherical	10-70	RAMESH, 2015
<i>Eryngium bungei</i>	N/A	Spherical	60-80	MORTAZAVI- DERAZKOLA, 2021
<i>Eugenia stipitata</i> <i>McVaugh</i>	Citric acid, malic acid, lutein Zeaxanthin, and beta carotene.	Spherical	15-45	KUMAR, 2016
<i>Ficus hispida f.</i>	Phenolic compounds, triterpenic acid	Spherical	20	RAMESH, 2018
<i>Fucus gardeneri</i>	Proteins, alkaloids, Flavonoids, polyphenols.	Spherical	19	PRINCY, 2021
<i>Lampranthus coccineus</i> <sup>1</sup> e <i>Malephora luea</i> <sup>2</sup>	Alkaloids, terpenoids, Flavonoids, phenols, glycosides, tannis	Both spherical	10-27 <sup>1</sup> 8-14 <sup>2</sup>	HAGGAG, 2019
<i>Licaria puchury- major</i>	Phenolic compounds, flavonoids	Triangular, truncated triangular and pseudo- spherical	57-60	GRAÇA, 2015
<i>Lotus lalambensis</i>	Proteins	Spherical	6-26	ABDALLAH, 2021

<i>Malva sylvestris</i>	Terpenoids	Spherical, hexagonal	20-40	ESFANDDARANI, 2018
<i>Mimusops elengi</i>	Flavonoids (Quercetin)	Spherical	20-300	BISWAL, 2021
<i>Morinda citrifolia</i>	Phenolic compounds, flavonoids, terpenoids	Spherical	30-55	SUMAN, 2013
<i>Nephelium lappaceum</i>	Anthocyanin, elleagic acid, syringic acid, and ellagitannin	Triangular, hexagonal	136	KUMAR, 2015
<i>Nigella arvensis</i>	Flavonoids, alkaloids, phenolic compounds, and proteins	Spherical	3-37	CHAHARDOLI, 2018
<i>Ocimum americanum</i>	Flavonoids	Spherical	48	MANIKANDAN, 2021
<i>Parkia biglandulosa</i>	Proteins, flavonoids	Spherical	15	JOHN, 2021
<i>Peganum harmala</i>	Phenolic compounds	Spherical	184	ALOMAR, 2020
<i>Phyllanthus emblica</i>	N/A	Spherical	60-80	DHAR, 2021
<i>Plantago major L.</i>	Phenolic compounds, proteins	Spherical	10-20	SUKWEENADHI, 2021
<i>Pongamia pinnata</i>	Flavonoids, carbohydrates, proteins, and alkaloids	Spherical	38	PAUL, 2019
<i>Propolis farcta</i>	N/A	Spherical	10	MIRI, 2015

<i>Quercus infectoria</i>	Alkanes, aromatic compounds	Spherical	29-38	KHATAMIFAR, 2021
<i>Rivina humilis</i>	N/A	Spherical	51	RAGHAVI, 2021
<i>Sideritis argyria</i>			115	
<i>Sideritis brevidens</i>	Phenolic compounds (chlorogenic acid)	Spherical	189	CEYLAN, 2021
<i>Sideritis lycia</i>			160	
<i>Syngonium podophyllun</i>	Proteins	Spherical	25	NAAZ, 2021
<i>Tagetes erecta</i>	Phenolic compounds	Spherical	24-49	KATTA, 2021
<i>Tasmanian flax-lily</i>	N/A	Spherical	70	AHMED, 2021
<i>Vigna mungo</i>	Flavonoids, phenolic compounds, polyphenols.	N/A	58-73	VARADAVENKATESAN, 2017
<i>Withania somnifera</i>	Flavonoids	Spherical	70-100	MARSLIN, 2015
<i>Zingiber officinale</i>	Phenolic compounds, flavonoids	Spherical	12-30	WANG, 2021

N/A = Not Available

Source: (Author, 2022).

### 3. MATERIALS AND METHODS

Silver nitrate (Sigma Aldrich, purity > 99%), sodium hydroxide (Sigma Aldrich, purity > 99%), hydrochloric acid (Sigma Aldrich, purity > 99%), and distilled water were employed throughout the reactions. Mueller Hinton agar and broth, and *S. Aureus* (CCCD-S009) and *E. Coli* (CCCD-CC01) were used for the antibacterial characterization.

The fruits of the guaraná plant (*Paullinia cupana*) were collected in Maués, a city located 259 km from Manaus, Amazonas, Brasil. The guaraná seed skins were taken out from the seeds and washed 3 times with distilled water to remove impurities. Then, they were exposed to drying under sunlight for 12h. The dried material was stored in plastic bags, insulated.

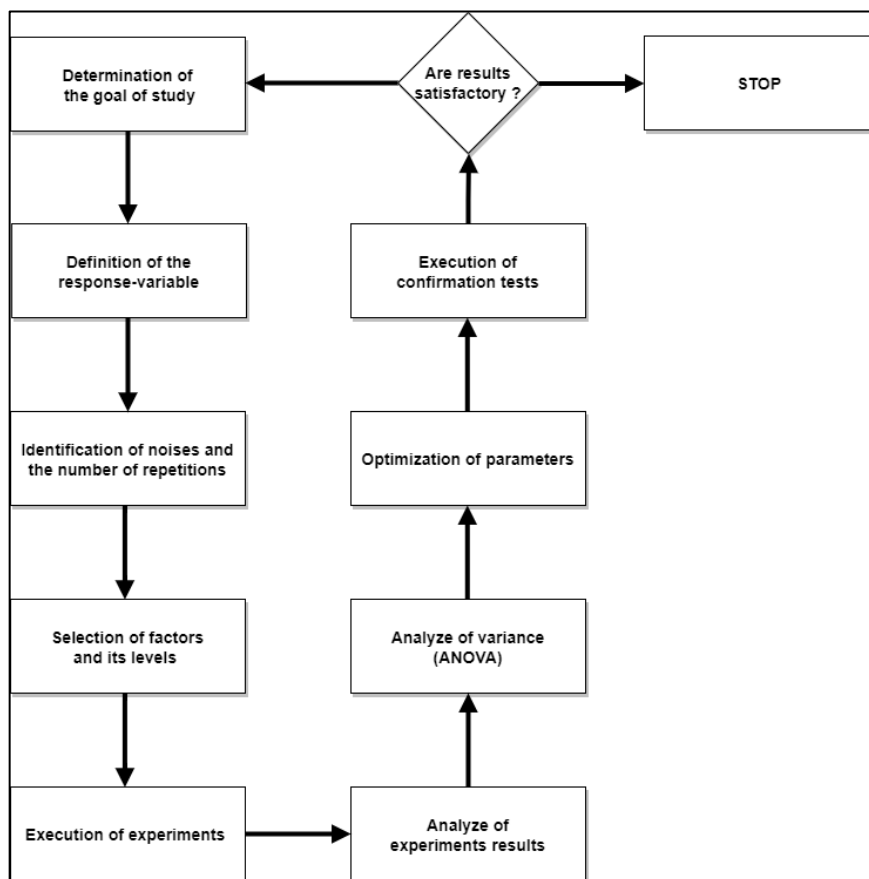
#### 3.1 OPTIMIZATION OF SYNTHESIS PARAMETERS

The Taguchi design method was applied to optimize the synthesis of silver nanoparticles. This method is applied as a robust tool to reduce the number of experiments, as well as to save raw material consumption (MONTGOMERY, 2012). In this case, it is possible to identify the optimal conditions and select the parameters that most influence the response variable. (KIM, S. et al, 2009). In Figure 9, it is possible to identify the main steps of the method.

Firstly, it is important to analyze all variables in the experiments defining what noise is and what variable is possible to control. The second action is to determine the response variable, in other words, the response for different conditions in the experiment. Selecting the control factor and uncontrolled factors, defining the factor and the levels. After the experiments, it is mandatory to analyze the results of experiments using statistic models such as analysis of variance (ANOVA) to identify which variables most influence the results and select the optimum point. (VALENTE, 2017)

Using the Taguchi method, it is possible to obtain the so-called signal-to-noise (S/N) ratio or index, which corresponds to the best adjustment that minimizes the variability to the noise in relation to the average value given. (GOMES, 2006)

Figure 9 - Taguchi method used for the optimization of synthesis parameters.



Source : (Author, 2022)

In this case, 9 runs were performed selecting four factors (pH, temperature, guaraná extract concentration, and silver nitrate concentration) with three levels each. The size of silver nanoparticles was selected as a response variable, as shown in Table 3.

Table 3. AgNPs synthesis parameters (factors) and their levels.

<b>Factors</b>	<b>Level 1</b>	<b>Level 2</b>	<b>Level 3</b>
<b>pH</b>	5	7	11
<b>Reaction temperature (°C)</b>	40	50	60
<b>Guaraná seeds extract concentration (mass/volume %)</b>	1	3	5
<b>Silver nitrate concentration (mM)</b>	1	5	10

A Taguchi orthogonal array L9 ( $3^4$ ) and the associated S/N ratio with the option “the smaller the better” was chosen to achieve the smallest size of AgNPs, as presented in Table 4.



Table 4. Taguchi's L9 orthogonal array.

Run	Factors				Response Variable
	pH	Temperature (°C)	C <sub>g</sub> (%)	C <sub>AgNO<sub>3</sub></sub> (mM)	AgNPs size (nm)
#1	1	1	1	1	-
#2	1	2	2	2	-
#3	1	3	3	3	-
#4	2	1	2	3	-
#5	2	2	3	1	-
#6	2	3	1	2	-
#7	3	1	3	2	-
#8	3	2	1	3	-
#9	3	3	2	1	-

A statistical analysis of the experimental data was performed using comprehensive software (Minitab 17) with 90 % ( $p > 0.1$ ) as the level of confidence. A 3D surface was plotted using Statistic software 10.

### 3.2 PROCESSING METHODS

Firstly, guaraná seed skins were ground to reduce the size through dry ball milling for 1 h. Using mechanical vibration, the particles were separated according to their size. The extractions were prepared by adding (1, 3, 5 g) of the extract of seed skins in 100 mL of water pre-heated at 60°C in 3 different Erlenmeyer flasks by the infusion method. After 20 min, the solution was filtered using Whatman #1 filter paper. Then, the guaraná seed skins extract was stored to be used in the next analyses.

An aqueous solution of silver nitrate (AgNO<sub>3</sub>) was added in an Erlenmeyer (125 mL) and placed in a magnetic stirrer with heating (IKA, C-MAG HS 10). According to the conditions of each run, the required temperature was adjusted, and the guaraná seed skins extract was added in droplets with constant agitation. The reaction was kept for 24 h. Photoactivation of AgNO<sub>3</sub> was avoided surrounding aluminum paper in the Erlenmeyer. A sample of 100 µL was collected in the first hour, and after 24 h, confirming the presence of AgNPs by UV-Vis.

After the synthesis, AgNPs were centrifugated at 6000 rpm for 20 min. Then, the colloidal solution was washed with deionized water. In the third wash, the supernatant was stored for further analyses and the precipitated was stored in an ultrafreezer for 24 h. Finally, the precipitate was lyophilized (LJJ freeze dryer) and the sample was kept for the remaining analyses. A semi-analytical balance (Bel Engineering, MG124A) was used to measure the final weight of the sample.

### 3.3 CHARACTERIZATION METHODS

A visual inspection of the AgNPs suspension was carried out. It is known that metallic nanoparticles such as copper, gold, and silver exhibit an ability of color change caused by surface plasmonic surface (SPR). This phenomenon is associated with the interaction of the light with the material in which the electric field resulting from the incidence of an electromagnetic light causes a collective oscillation of electrons present on the dielectric surface of nanoparticles. Thus, the absorbance in the visible region of the spectrum can assume different colors depending on the analyzed metal, size, and shape of the nanoparticle. For silver nanoparticles, the color changes from transparent to dark brown. (KANCHI, 2018) (BARBOSA, 2018).

Moreover, analytical equipment was used for the characterization of the synthesis materials and products, as listed in Table 5 and detailed right after.

Table 5. Equipment used in the synthesis and characterization of AgNPs.

<b>Equipment</b>	<b>Manufacturer</b>	<b>Model</b>
DLS and zeta potential	Malvern	Zeta/Nanosizer
FTIR	Agilent	Cary 630
pHmeter	QualXtron	QX110
SEM	JEOL	JSM IT500HR
TEM	JEOL	1400 Flash
UV-Vis	Shimadzu	UV-1800
XRD	Bruker	D2 Phaser
ICP-OES	Shimadzu	ICPE-9820
DI-ESI-MS	Thermo Scientific	LCQ fleet
XRF	Philips	PW 2400

### 3.3.1 X-Ray Fluorescence

The quantitative chemical analyzes of 20 grams of guaraná seed skins were carried out in a Philips, model PW 2400, with a 3 kW tube and rhodium target. The losses on fire was determined by burning the samples for 1 h at 1000 °C.

### 3.3.1 Inductively coupled plasma atomic emission spectroscopy (ICP-OES)

It was possible to measure the concentration of silver nanoparticles using Inductively coupled plasma atomic emission spectroscopy (ICP-OES) in which was performed in triplicate ( $25\text{ °C} \pm 1\text{ °C}$ ). The samples of silver nanoparticles were diluted in proportion (1:20) to water. Then, the colloidal solution was kept in dark condition in order to avoid the oxidation reaction of the silver nanoparticles.

### 3.3.1 Direct-injection Electrospray Ionization Spectroscopy Mass Spectrometry (DI-ESI-MS)

The analysis of DI-ESI-MS was carried out by ion trap masses (LCQ Fleet from Thermo Scientific) equipped with a source of electrospray ionization (ESI), operating in positive mode from the Laboratory of Chromatography and Mass Spectrometry - LABCEN of the Central Analytics/UFAM. To obtain MS/MS spectra, energies were used collision between 20-35 eV.

The m/z range analyzed was 100-600 Da. The extracts were prepared com methanol (HPLC grade) at 10 ppm. The data were processed through the program *Xcalibur 2.0.7*.

### 3.3.2 Ultraviolet-Visible-Spectroscopy (UV-Vis)

The absorbance of silver nanoparticles was measured using UV-Vis at a wavelength of 190-700 nm to identify the presence of silver nanoparticles and their dispersity. For AgNPs, the absorption peaks are usually between 400-500 nm wavelength.

### 3.3.2. Dynamic Light Scattering (DLS)

Using the DLS technique, it is possible to determine the hydrodynamic size of nanoparticles, and polydispersity index as well as the zeta potential to measure the colloidal stability. The particle size distribution was obtained by the scattering technique light dynamics (DLS) using a MALVERN particle size analyzer (ZetasizerNanosizer) from the Interdisciplinary Laboratory for the Development of Nanostructures (LINDEN) from UFSC. Before analysis, AgNPs samples were dispersed in distilled water in an ultrasound bath for 1h.

### 3.3.3. Fourier-Transform Infrared Spectroscopy (FTIR)

The lyophilized AgNPs were analyzed by the FTIR to identify compounds from guaraná extract responsible for reducing and stabilizing the silver nanoparticles. For comparison, a sample of the guaraná seeds skin extract was analyzed in diffuse reflectance mode in the length from 500 to 400  $\text{cm}^{-1}$  with a resolution of 8  $\text{cm}^{-1}$  at 25  $^{\circ}\text{C} \pm 1^{\circ}\text{C}$ .

### 3.3.4. X-Ray Diffraction (XRD)

The crystallinity, crystal size, and the chemical structure of AgNPS can be determined by XRD in which the scattering of X-rays on the atoms of a crystal and the diffraction of the crystal provides information about the structure of atoms in the solid. (RANA, 2020). The obtained diffractograms were compared with the pattern reported in the crystallographic record JCPDS (Joint Committee on Powder Diffraction Standards) using the X'pert HighScore Plus software. The average crystalline size was calculated using the Debye-Scherrer equation

$$D = \frac{k \lambda}{\beta \cos \theta}$$

where  $D$  represents the average crystalline size of nanoparticles,  $k$  is a geometric factor (0.9),  $\lambda$  is the wavelength of the X-ray radiation source and  $\beta$  is the angular FWHM (Full-width at half maximum) of the XRD at the diffraction angle  $\theta$ .

### 3.3.5. Scanning Electron Microscopy (SEM) and Transmission Electron Microscopy (TEM)

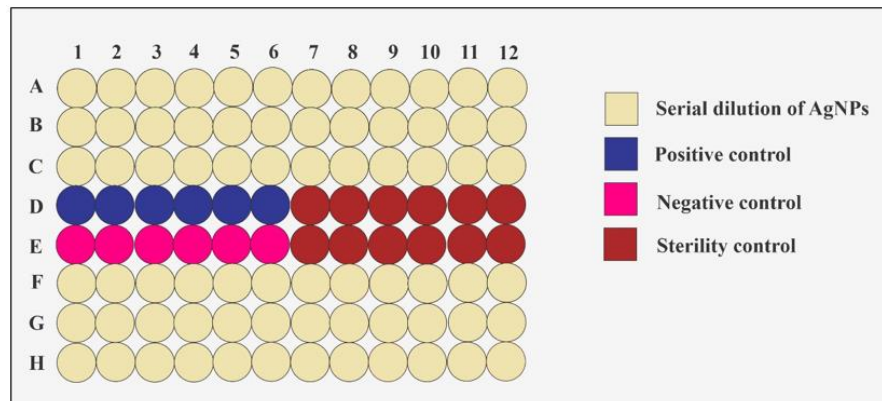
SEM images were taken to reveal the morphology of the biosynthesized AgNPS including specific information about the internal structure. Lyophilized silver nanoparticles were metalized with platinum. TEM samples were prepared using the supernatant (third wash). After drying for 8 h, the samples were set on a copper grid with formvar paper. Using TEM, it is possible to determine the particle size and its distribution, as well as the shape of the AgNPs using Image J software. In parallel, the results can be compared with those obtained by the DLS technique.

### 3.4 ANTIBACTERIAL ACTIVITY EVALUATION

The antibacterial activity of the AgNPs was evaluated in two methods. The first method was using the agar diffusion technique for gram-positive *Staphylococcus aureus* (CCCD-S009) and gram-negative *Escherichia coli* (CCCD-E005). The sample was tested by the agar diffusion methodology, according to the Clinical Laboratory Standards Institute CLSI (2011), against the same strains mentioned. The microbial suspension was made in 0.85% saline solution until reaching the 0.5 mark on the McFarland scale. With the aid of a sterile swab, the bacterial suspensions were seeded on Müeller Hinton agar. Subsequently, wells were made on the surface of the agar, where 100  $\mu$ L of the test sample was inserted, as a negative control, only the guaraná seed skins extract without the nanoparticle was used and the positive control was Levofloxacin 250  $\mu$ g/mL for the bacteria. The plates were closed and incubated at 37°C for 24 h. After this period, it was observed if there was the formation of inhibition halos which were measured with the aid of a caliper

The minimum inhibitory concentration (MIC) (Figure 10) was determined by using 96 wells titer plate by broth microdilution technique observing the reduction of resazurin (7-hydroxy-3H-phenoxazin-3-one 10-oxide).

Figure 10 - Broth microdilution method using 96 well-plates.



Source: (Author, 2022).

The mechanism is based on the reduction of resazurin (blue) which indicates the absence of bacterial growth to resorufin (pink) which indicates the presence of bacterial growth. The samples were tested against strains purchased commercially (Cefar Diagnóstica). The assay was performed using a sterile 96-well microplate where 100  $\mu\text{L}$  of the microbial inoculum at a concentration of  $5 \times 10^5$  CFU/mL was inserted in triplicate for the bacteria with 100  $\mu\text{L}$  of AgNPs. The positive control used for both bacteria was Levofloxacin 250  $\mu\text{g}/\text{mL}$ . As a negative control, the microbial inoculum and guaraná seed skins extract were inserted and, for sterility control, 100  $\mu\text{L}$  of the sterile culture medium was used for the preparation of the inoculum (Mueller Hinton). Subsequently, the plates were incubated at 37°C for 24 h (bacteria) in a BOD (Biochemical Oxygen Demand) oven. After this period, 30  $\mu\text{L}$  of resazurin were inserted into all wells of the antibacterial activity assay plates. The plates were incubated again at 37°C for 1 to 2 h to verify the reduction of inserted developers. For the antibacterial assay, the pink color is indicative of cell growth, that is, without antimicrobial action.

## 4. RESULTS AND DISCUSSIONS

### 4.1 OPTIMIZATION OF SILVER NANOPARTICLES SYNTHESIS

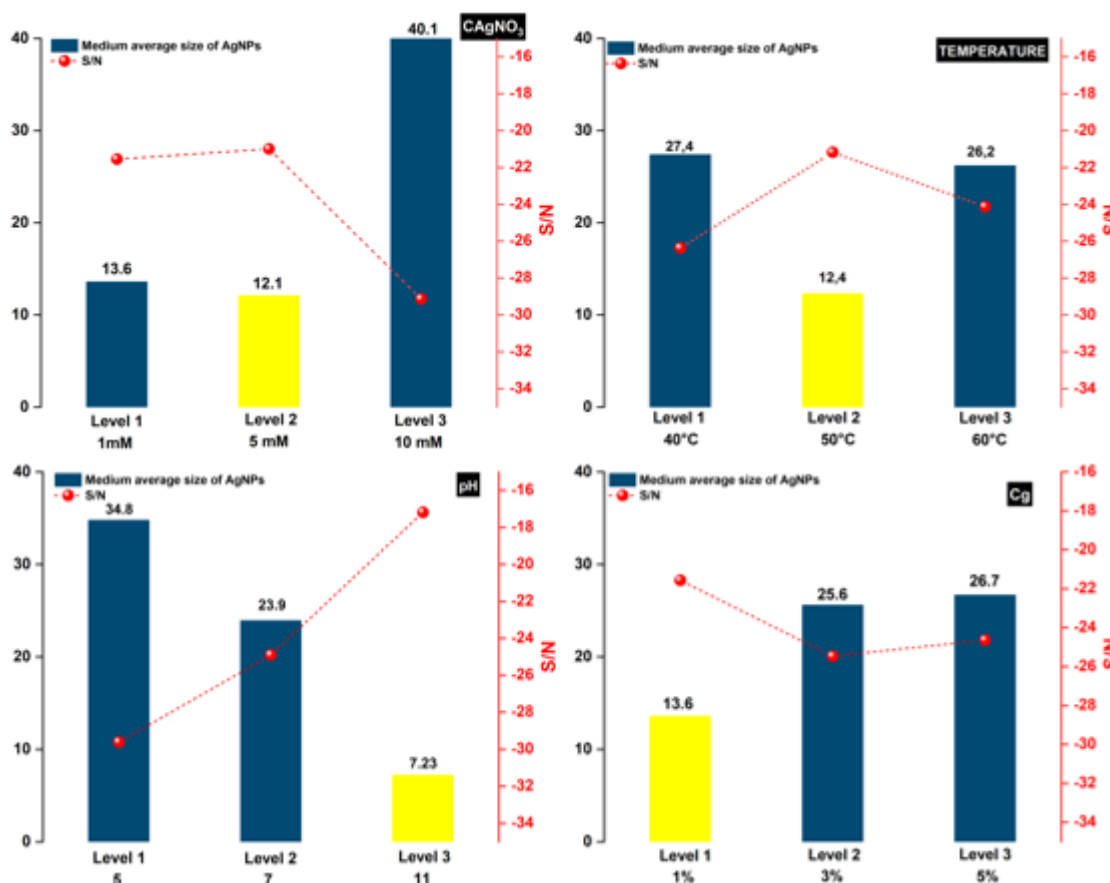
According to the Taguchi Design, 9 experiments were carried out in a random order according to the conditions described in Table 6. An efficient antibacterial activity is achieved using AgNPs of the smallest size. For this proposal, the average size of AgNPs was analyzed as a response variable:

Table 6. Optimization of parameters in the synthesis of AgNPs.

Run	pH	Temperature (°C)	C <sub>g</sub> (%)	C <sub>AgNO<sub>3</sub></sub> (mM)	Average Size (nm)	S/N
#1	1	1	1	1	23.5	-27.42
#2	1	2	2	2	19.0	-25.57
#3	1	3	3	3	61.9	-35.83
#4	2	1	2	3	51.2	-34.19
#5	2	2	3	1	10.7	-20.59
#6	2	3	1	2	9.9	-19.91
#7	3	1	3	2	7.5	-17.50
#8	3	2	1	3	7.4	-17.38
#9	3	3	2	1	6.8	-16.65

The main effects plots were used to investigate the relationship between the factors and the response variable as shown in Figure 11.

Figure 11 - Influence of single factors on the average size of AgNPs and respective signal-to-noise ratio (S/N): concentration of silver nitrate ( $C_{AgNO_3}$ ), temperature of the reaction, concentration of guaraná seeds skins extract ( $C_g$ ), and pH.



It is possible to notice that the interpretation of plot S/N ratio is opposite when compared to the main effect plot. Also, the best level of each factor was chosen according to the highest S/N ratio.

Thus, a decrease in  $AgNO_3$  concentration from 13.6 mM (Level 1) to 12.1 mM (Level 2) generates a smaller average of AgNPs size, which may be associated with an unbalance among the amounts of reactant and reducing agent. Also, the value of the average size of AgNPs increased from 12.1 to 40.1 nm, as the  $AgNO_3$  concentration increased from 5 mM (Level 2) to 10 mM (Level 3). This may be attributed to the higher availability of  $Ag^+$  at higher  $AgNO_3$  concentrations contributing to a faster rate in the bioreduction reaction. These results are in accordance with HTWE (2019) in which AgNPs were synthesized using *Imperata cylindrical* extract and a diameter of 32.70 nm was achieved using  $AgNO_3$  concentration of 0.5 mM, but using  $AgNO_3$  concentration of 0.9 mM, the AgNPs diameter was higher with 39.91 nm.



At a higher extract concentration, larger clusters of particles might be formed resulting by increasing the average concentration from 1% (Level 1) to 10% (Level 3). An increase in the size of AgNPs was reported by AHMED (2021) when the plant extract concentration increases.

The size of AgNPs has been proved to be a temperature-depend process, as well as the effect of temperature on the size of AgNPS is directly dependent on the kinetic reaction (LEE, 2014). It is reported that nanoparticles grow faster at higher temperatures (LIU, 2020). It is noted that the AgNPs size increases with the temperature from 12.4 nm (50 °C, Level 2) to 26.2 nm (60 °C, Level 3). It was reported by JIANG (2011) similar observation about temperature and the size of AgNPs. In their work, AgNPs were higher in size when a higher temperature was applied. However, in Level 1 (40 °C), the size of the nanoparticles decreases from 27.4 to (12.4, Level 2) nm which may be associated with insufficient precursors present in the reaction. Similar behavior was observed by LIU (2020) in which at high temperature (90°C), AgNPs were obtained with lower size when compared to those produced at a lower temperature. Also, KHALIL (2014) reported that by increasing the temperature of the reaction, a rapid reduction rate of silver ions can lead to homogeneous nucleation of silver obtaining a small size of AgNPs.

The pH is another factor that affects the shape, morphology, and size of the AgNPs (MELKAMU, 2021). Increasing the pH from 5 to 7, the average size of AgNPs decreases from 34.8 nm (Level 1) to 7.23 nm (Level 3). It was reported that in an acid medium, there is a weaker nucleation process and a poor process of stabilization in the production of AgNPs resulting in a higher nanoparticles size (KHALIL, 2014). In an alkaline medium, the rapid nucleation process occurs due to the availability of functional groups in the guaraná seeds skins, such as alkaloids (caffeine, theophylline, and theobromine).

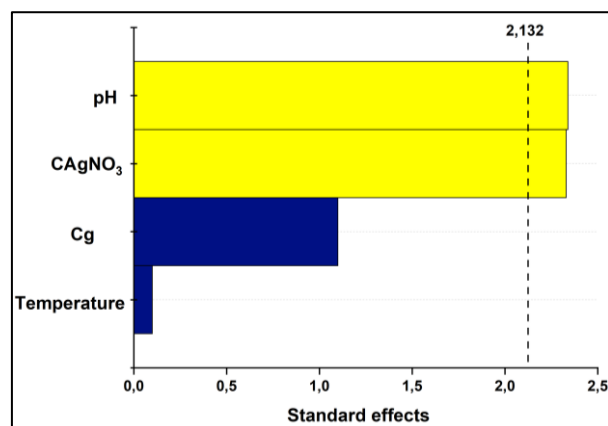
The results of ANOVA analysis of the factors that affect the average size of silver nanoparticles are listed in Table 7.

Table 7. Analysis of variance (ANOVA) of the regression equation of size of AgNPs.

Source	D.F	Seq SS	Adj MS	P-Value	Contribution (%)
<b>Regression</b>	4	2548.5	637.1	0.153	75.30
<b>pH</b>	1	1151.5	1151.4	0.079	34.02
<b>Temperature (°C)</b>	1	2.16	2.16	0.924	0.06
<b>C<sub>g</sub> (%)</b>	1	257.4	257.4	0.329	7.61
<b>C<sub>AgNO<sub>3</sub></sub> (mM)</b>	1	1137.5	1137.5	0.080	33.61
<b>Error</b>	4	835.9	835.9	-	24.70
<b>Total</b>	8	26814.1	-	-	100.00

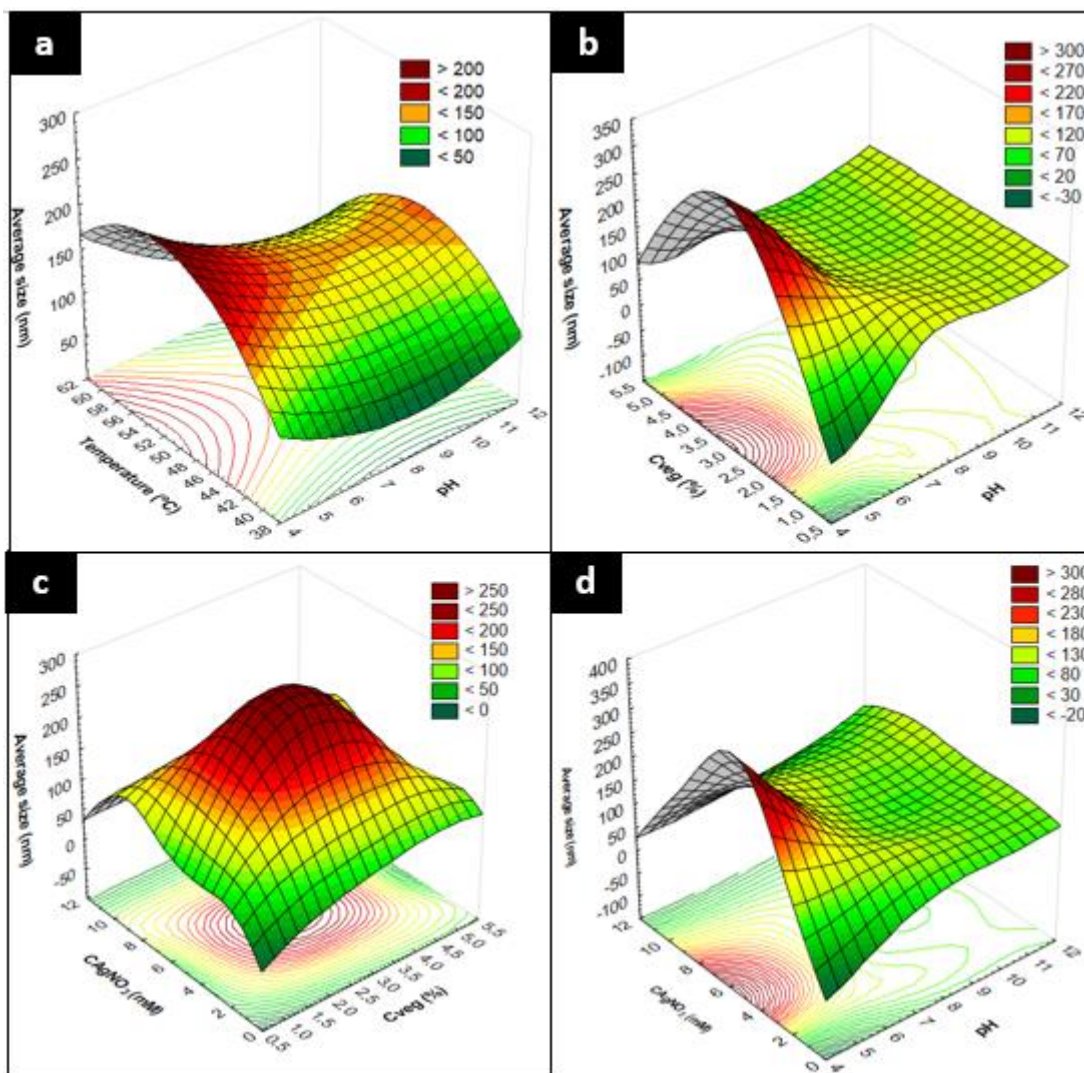
The main variable that significant contribution was the pH when compared to the other factors being evidenced by the contribution of 34.02% followed by silver nitrate concentration (33.61%) while seeds extract concentration (7.61%) and temperature (0.06%) had insignificant effects on these results. In addition, it is evidence of an expressive error (24.70 %) caused by noise on the measurement of particle size.

The Pareto chat (Figure 12) shows 2 significant factors affecting the average size of AgNPs. The pH was the most significant factor followed by silver nitrate concentration and by the seed skins guaraná extract and the temperature. Probably, the levels selected of the guaraná seed skins extract and the temperature were very close, and a variation of these parameters was not sensitive enough to cause a significant impact on the average size of AgNPs.

Figure 12 - Pareto chart of the standardized effects (Response in size (nm)  $\alpha = 0,1$ ).

Thus, a three-dimensional (3D) surface plot of the factors ( $C_{AgNO_3}$ , temperature, pH, and  $C_g$ ) is shown in Figure 13 to present the respective influences on the average size of AgNPs:

Figure 13 - Response surfaces in relation to the average size of AgNPs: concentration of silver nitrate ( $C_{AgNO_3}$ ), temperature of reaction, concentration of guaraná seed skins extract ( $C_g$ ), and pH.



From S/N ratio and ANOVA, the optimized conditions at AgNO<sub>3</sub> at 0.005M (Level 2), pH at 11 (Level 3), temperature of reaction at 50°C (Level 2), and guaraná seed skins extract concentration of 1% (m/v) (Level 1) exhibited a smaller size. Thus, this sample was selected by Taguchi Design to be chemically characterized and used in the antibacterial activity test.

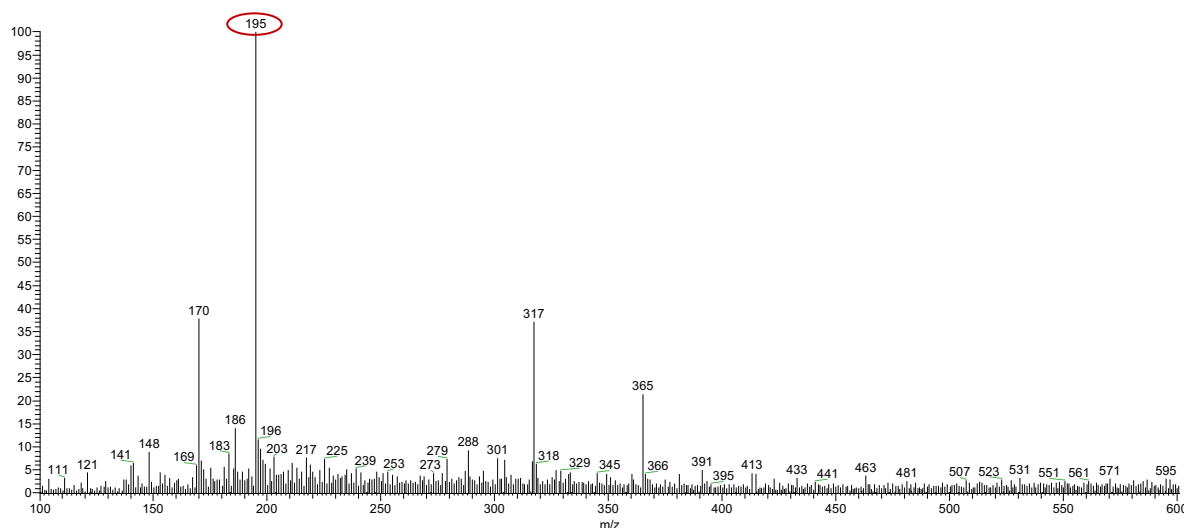
## 4.2 CHARACTERIZATION OF SEED SKINS GUARANÁ

### 4.2.1 Chemical profile of extract by Direct Infusion Electrospray ionization mass spectrometry (DI-ESI-MS)

The fingerprints mass spectra of samples of guaraná seed skins extract in positive mode in 100-600  $m/z$  (Figure 14). Thus, the result of DI-ESI-MS technique, the chemical profile of aqueous extract guaraná seed skins was investigated and led to the tentative identification of caffeine as possible majority compound.

According to the study of Mclellan et al. (2012), extracts of seeds from the fruit of guaraná indicates caffeine high concentrations (2-15%) of the dry weight. Moreover, caffeine was the major compound with a concentration of 4% found by Roggia et al. (2020). In this case, the quantification of compounds present in powdered guaraná extract was carried out using a validated HPCL method.

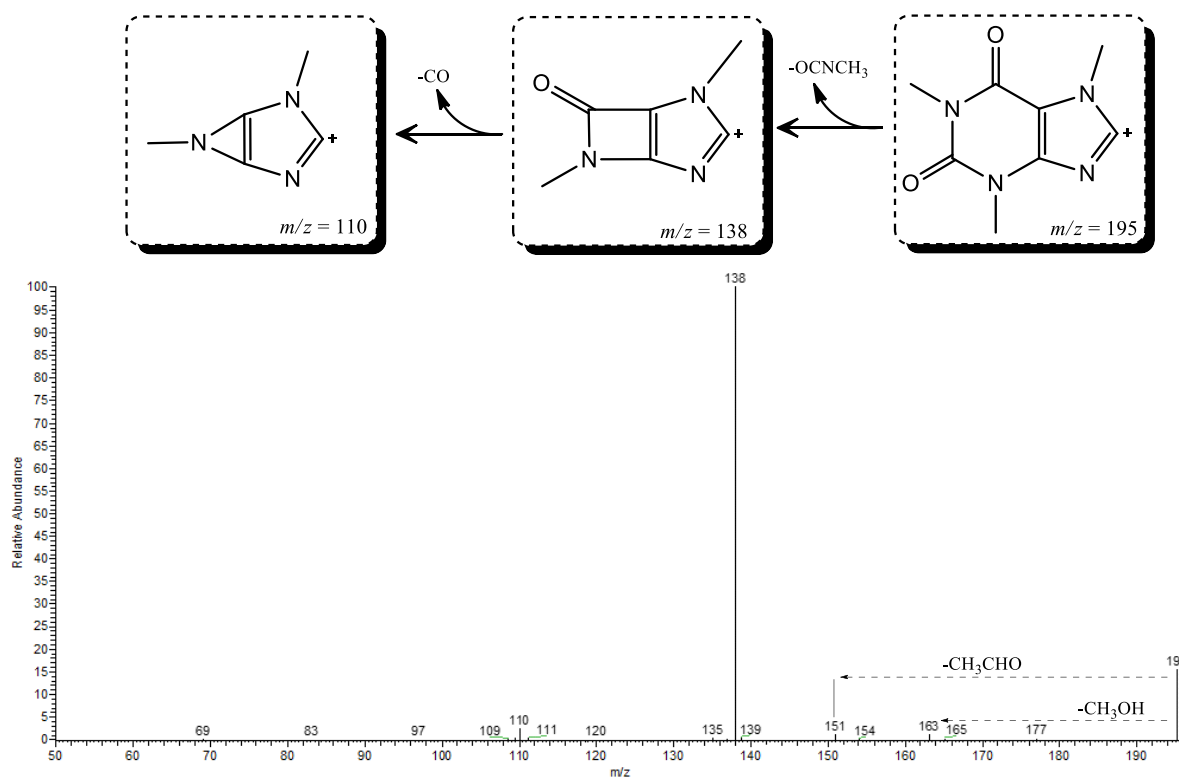
Figure 14 – DI-ESI-MS fingerprints of guaraná seed skins extract in a positive mode in 100-600  $m/z$



Besides  $m/z^+$  195 peaks, several other ions (e.g.  $m/z^+$  170; 317; 365) with high relative intensity were observed in the seed skins guaraná extract, which can be related to alkaloids compounds, suggesting these extracts as complex matrices. This way, more studies are necessary to determine the chemical composition using alternative techniques such as High-Performance Liquid Chromatography (HPLC) and Nuclear Magnetic Resonance (NMR) in order to help to identify compounds present in these matrices.

The MS/MS spectrum of the ion at  $m/z$  195 showed a base peak at  $m/z$  138 and less intense ions at  $m/z$  163, 151, and 110 (Figure 15) which are in agreement with the structure of caffeine (BIANCO, 2009).

Figure 15 – Proposed products ions spectra of fragmentation of caffeine in peak at  $m/z$  195.



The spectrum of protonated caffeine at ion  $m/z$  195 displayed an initial loss of 57 Da ( $O-CNCH_3$ ) by retro-Diels Alder rearrangement. In addition, a base peak at  $m/z$  163 showed a loss of 32 Da ( $CH_3CH=O$ ). Moreover, at  $m/z$  151 a loss of 44 Da ( $CH_3CH-O$ ) and lastly, the loss of carbon monoxide ( $CO$ ) ( $m/z$  138  $\rightarrow$  110) were detected. Thus, caffeine was detected in the chemical composition of the guaraná seed skin extract.

#### 4.2.2 X-ray fluorescence (XRF) of seed skins guaraná (*Paullinia cupana*)

The oxides present in the seed skins of guaraná are shown in Table 9.

Table 9 – Chemical analysis as oxides of guaraná seed skins by X-ray fluorescence.

Oxides	Composition (%)	Literature (MAIA, 2022)
K <sub>2</sub> O	0.918	42.204
CaO	0.487	26.831
SiO <sub>2</sub>	0.478	1.815
Al <sub>2</sub> O <sub>3</sub>	0.383	0.000
P <sub>2</sub> O <sub>5</sub>	0.211	9.845
MgO	0.112	2.902
SrO	0.054	-
Na <sub>2</sub> O	<0.05	-
Fe <sub>2</sub> O <sub>3</sub>	<0.05	1.571
TiO <sub>2</sub>	<0.05	-
BaO	<0.05	-
Co <sub>2</sub> O <sub>3</sub>	<0.05	-
Cr <sub>2</sub> O <sub>3</sub>	<0.05	-
PbO	<0.05	-
MnO	<0.05	-
ZnO	<0.05	-
ZrO <sub>2</sub> /Hf	<0.05	-
Loss on Fire (LOF)	97.417	-

The main chemical elements found in the guaraná seeds' skin were potassium oxide (K<sub>2</sub>O), calcium oxide (CaO), and silicon dioxide (SiO<sub>2</sub>) with 97.417% LOF.

These results are similar to those of Maia et al. (2022), who identified the same major oxides in guaraná seed skins. The difference between both results is based on the region where the seed skins were collected, the stress caused by the environment, and biological factors.

The chemical composition of seed skins guaraná is very important in order to identify the compounds present around the silver nanoparticles in further analysis and elucidate a

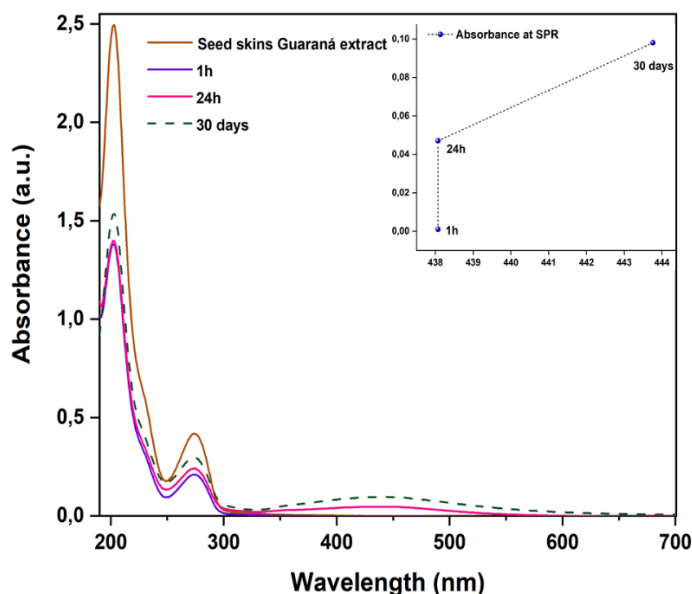
hypothetical mechanism between some compounds from seed skins guaraná and biogenic AgNPs.

### 4.3 CHARACTERIZATION OF SELECTED SILVER NANOPARTICLES

#### 4.3.1 UV-VIS Spectroscopy

The extract of guaraná seed skins was hypothesized to be an efficient reduction and capping agent in the synthesis of AgNPs. As shown in Figure 16, the evolution of the synthesis of AgNPs was enhanced at longer reaction times as verified by the broad range between 400-500 nm wavelength.

Figure 16 - Absorption spectra of AgNPs observed in 1 h, 24 h, and 30 days of reaction.

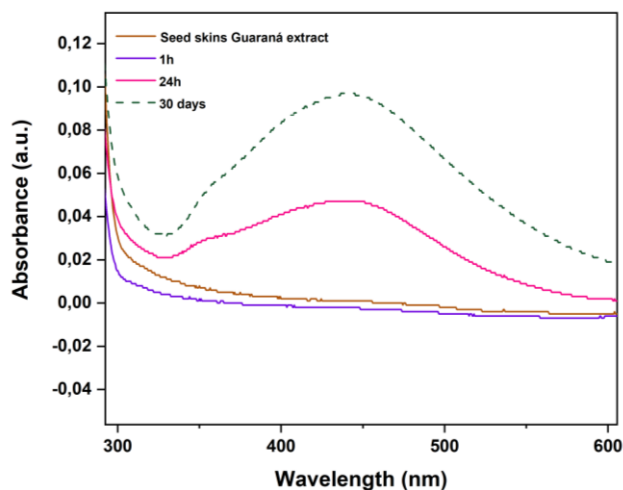


In UV-vis absorption spectra, the guaraná extract shows two absorption bands. A strong band at 250-290 nm may be originated from the A ring benzoyl system, and a band at 190-250 nm is associated with the cinnamoyl system (FENG, 2017). Also, the reduction of the value absorption peak of the extract is due to its ability to the reduction of  $\text{Ag}^+$  to the silver nanoparticles ( $\text{Ag}^0$ ).

In the first hour of reaction (Figure 17), it is not possible to visualize any absorption band typical of the silver nanoparticles (400-500 nm). After 24 h, Surface Plasmonic Resonance (SPR) absorption peak is present between 350-500 nm is shown, which denotes the presence of stabilized AgNPs in the colloidal dispersion.

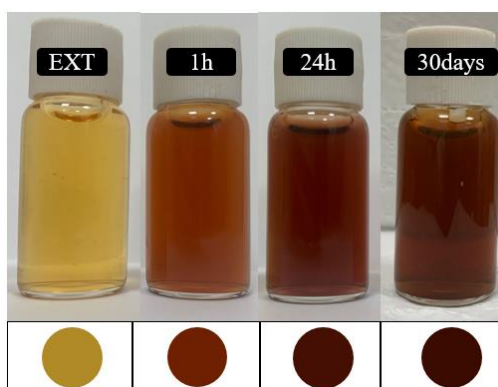
After 30 days, a slight increase of SPR peak intensity is visible indicating not only the presence but a good stabilization of AgNPs, which suggests no aggregation during this period. Besides, The initial absorption peak of 438 nm was found to be 443 nm after 30 days. A red shift signifies an increase in the average size of AgNPs (MUNIYAPPAN, 2014).

Figure 17 - AgNPs SPR peak intensity.



In addition, the appearance of this band and the color change to yellowish brown (Figure 18) is due to the cumulative oscillation of the conducting metal surface electrons in resonance, indicated by  $\lambda_{\max}$  of 438 nm, which is typical for AgNP.

Figure 18 - Color change AgNPs (1 h, 24 h, and 30 days).



After a few hours, there was no change in the color solution indicating that the reduction process had been reduced (JAIN, 2017). After 30 days, the color has no significant change indicating no reaction at this time.

Morphological information about AgNPs can also be obtained by UV-Vis spectra (IBRAHIM, 2021). AgNPs produced were isotropic and spherical due to the presence of a

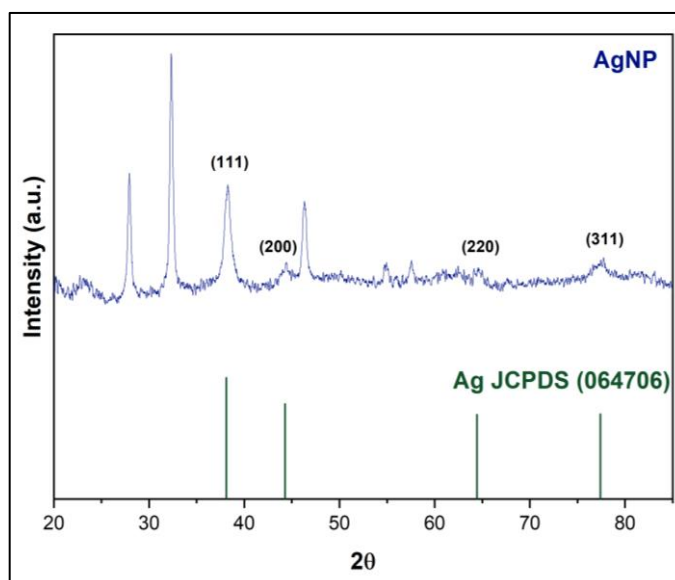


single surface plasmonic response peak which can be confirmed by TEM. The broadening of UV-vis suggests a polydispersity in nature, while in 24 h the value of absorbance achieves the highest value indicating more quantities of AgNPs. Thus, it is hypothesized that flavonoids, polyphenols, alkaloids present in the *P. Cupanna* seed skins extract act as reducing/stabilizing agents.

#### 4.3.2 X-ray Diffraction (XRD)

Additionally, XRD was performed to identify the crystalline or amorphous nature of AgNPs, as shown in Figure 19.

Figure 19 - XRD spectrum of AgNPs.



When compared with standard JCPDS (064706) for silver, the XRD pattern confirmed the presence of AgNPs. The spectrum shows peaks at  $2\theta$  values of 38.30, 44.44, 64.47, and 77.65, which correspond respectively to the (111), (200), (220), and (311) crystallographic planes of the face-centered cubic (*fcc*) configuration. Additional peaks were observed suggesting the presence of crystals of cristobalite ( $\text{SiO}_2$ ) at  $2\theta$  values of  $\sim 26$  and  $\sim 33$ , eventually from the *Paullinia Cupana* extract at the surface of the AgNPs (BAXTER, 1999). The XRD confirms the potential use of the extract to synthesize crystalline AgNPs.

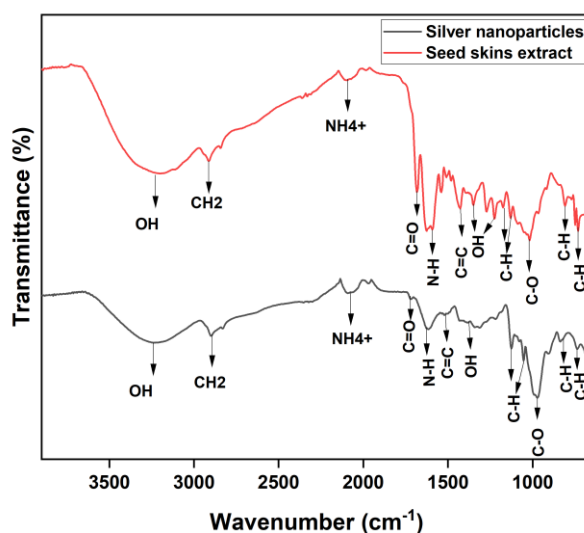
These results are consistent with those of Prema et al. (2022), who found cubic crystalline silver (111), (200), (220), and (311) crystallographic planes for AgNPs. Also, broader peaks indicate that the crystallite size is small (BINDHU, 2014). Based on the

crystalline peaks of AgNPs, the mean crystallite size was measured using the Scherrer equation being 18,55 nm. It is less in size when compared to the average size of AgNPs measured by DLS and TEM.

#### 4.3.3 Fourier-Transform Infrared Spectroscopy (FTIR)

FTIR was used to identify the functional groups present on the surface of AgNPs (Figure 20 and Table 10). The similarities with some marginal shifts in the peak between both spectra indicate the presence of the residual extract, which was involved in the capping, reducing, and stabilizing processes at the surface of AgNPs.

Figure 20 - FTIR spectra of the guaraná seeds skin extract and the as-prepared AgNPs.



Specifically, the IR spectrum of the extract presented a broad band at  $3214\text{ cm}^{-1}$  corresponding to the strong bond of  $\text{-OH}$  functional groups in alcohols and phenolic compounds. The band at  $2912\text{ cm}^{-1}$  corresponded to the C-H stretching vibration of methyl and methylene groups from the lipids in the extract. Moreover, the band at  $2092\text{ cm}^{-1}$  corresponds to amine salts  $\text{NH}_4^+$  stretching of amines, while the band at  $1682\text{ cm}^{-1}$  corresponds to the stretching  $\text{C=O}$  of a protein and/or ester. In addition, N-H bending of aromatic amines at  $1619\text{ cm}^{-1}$  was also observed. Additionally, the band at  $1348\text{ cm}^{-1}$  corresponds to OH bending corresponding to primary alcohols that might be from alkaloid compounds and  $1216\text{ cm}^{-1}$  is attributed to the stretching of aromatic amines. Lastly, the bands at  $1173$ ,  $1129$ ,  $800$ , and  $730\text{ cm}^{-1}$  are attributed to CH bending, which is typical of compounds of alkaloids and flavonoids present in the extract.

Similarly, FTIR spectrum of AgNPs showed 13 main peaks: 3264, 2899, 2067, 1720, 1628, 1517, 1378, 1367, 1125, 1058, 973, 836, 736  $\text{cm}^{-1}$ . When comparing the extract to the AgNPs spectra, slight changes were observed in the peak positions and intensities. AgNPs spectrum shows a strong absorption band at 3264  $\text{cm}^{-1}$  (OH stretching). Some bands observed in the extracts and AgNPs spectra revealed small differences eventually due to the crosslink between them. It suggests that the O-H and C=O groups of the biomolecules from seed skins extract are adsorbed on the surface of AgNPs and they are involved in the reducing/stabilizing processes.

Table 10. Bands in the FTIR spectra of guaraná seeds skin extract and as-prepared AgNPs.

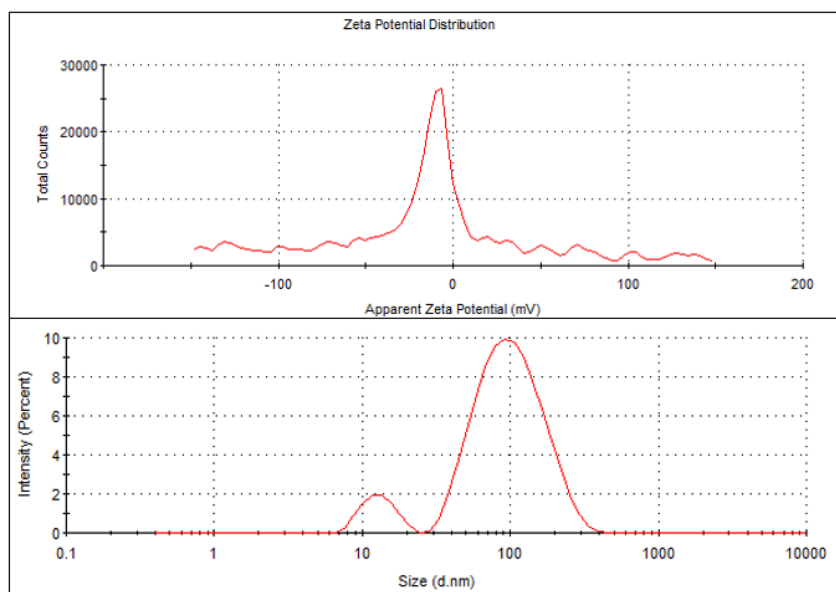
Wavenumber of seed skin extract ( $\text{cm}^{-1}$ )	Wavenumber of AgNPs ( $\text{cm}^{-1}$ )	Type of bond	Reference
3214	3264	OH stretching	(RAMESH, 2018)
2912	2899	CH <sub>2</sub> and CH stretching	(SINGH, 2017)
2092	2067	NH <sub>4</sub> <sup>+</sup> stretching	(SILVERSTAIN, 1962)
1682	1720	C = O stretching	(SING, 2017)
1619	1628	N-H bending (scissoring)	(MUTHKRISHNAN, 2015)
1417	1517	C=C stretching	(KUMAR, 2015)
1347	1378	C-N stretching	(JEMILUGBA, 2019; BALASHANMUGAM, 2015)
1216	1367	OH bending	(SILVERSTAIN, 1962)
1173	1125	C-H stretching	(SILVERSTAIN, 1962)
1129	1058	C-H stretching	(SILVERSTAIN, 1962)
1014	973	C-O stretching	(BALACHANDRAN, 2012; KUMAR, 2015)
800	836	C-H bending	(KHATAMIFAR, 2021)
730	736	C-H bending	(KHATAMIFAR, 2021)

It is important to remind that the extract used in this study is formed by alkaloids, flavonoids, terpenoids, and proteins, which have acted simultaneously as reducing/stabilizing agents. Similar observations were investigated by Rodríguez et al. (2021), who used agri-food waste in the synthesis of AgNPs as capping/stabilizing agents. In their study, proteins, polysaccharides, and phenolic compounds were reported as potential agents responsible for the reduction of  $\text{Ag}^+$  to  $\text{Ag}^0$ .

#### 4.3.4 Particle Size Distribution and Zeta Potential

The surface properties and stability of seed skins of guaraná (Figure 21) can be determined using zeta potential analysis by DLS. In general, zeta potential less than -30 mV or higher + 30mV exhibit good stability .

Figure 21 - Zeta potential and particle size distribution of AgNPs derived from guaraná seed skin extract.



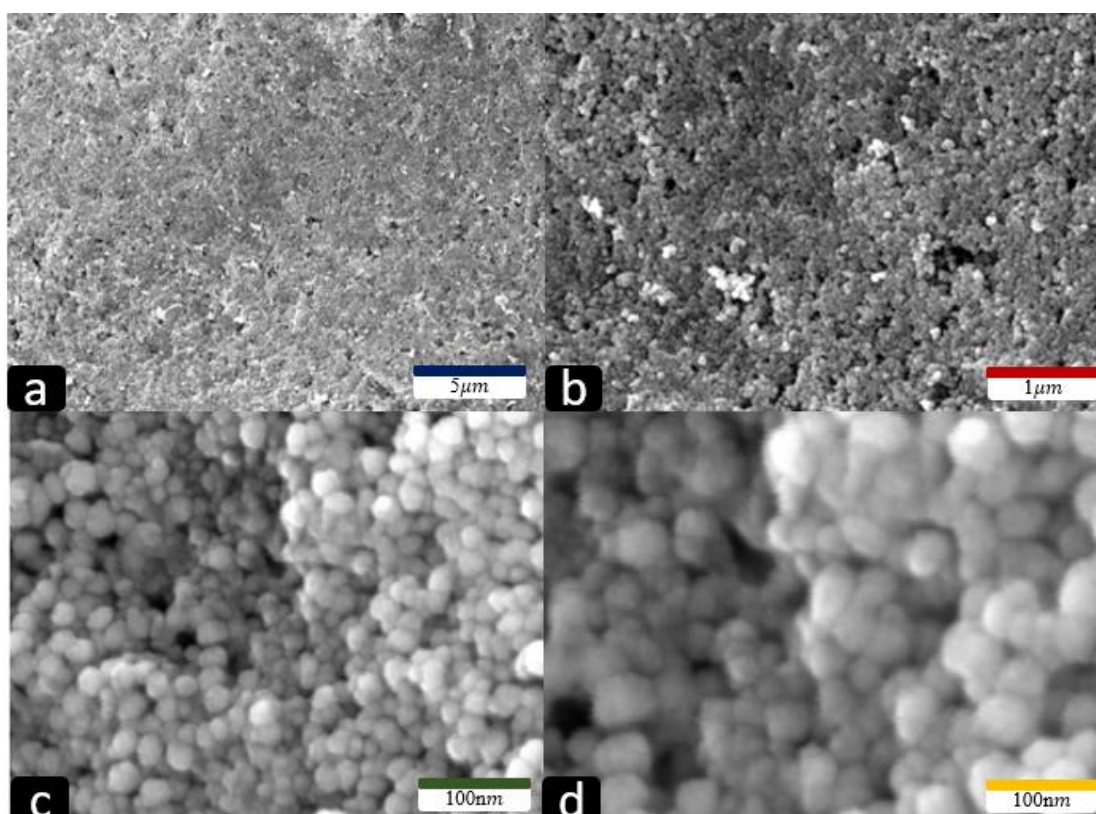
The average zeta potential of AgNPs was -11.2 mV with an average size of 63.9 nm ( $\pm 1.64$ ) and particle size distribution of 0.448. The negative value of zeta potential suggests a surface charge of guaraná seed skin extract might come from the  $\text{OH}^-$ ,  $\text{COO}^-$ ,  $\text{CO}^-$  functional groups identified in FTIR analysis. In this case, a negative charge on the surface of AgNPs prevents aggregation by the electrostatic and/or steric repulsion among the negative charges.

Similar results were found by Palithya et al. (2021) using flower extracts of *Aerva lanata* in green synthesis of AgNPs. In their work, a zeta potential of AgNPs of -18.7 mV was obtained indicating the presence of a negative charge on the surface of AgNPs.

#### 4.3.5 Microscopy Analyses (SEM and TEM)

SEM and TEM analyses were performed to investigate the morphology, size, and size distribution of AgNPs. SEM images at different magnifications are shown in Figure 22.

Figure 22 - SEM micrographs of AgNPs obtained by green synthesis using *Paullina Cupana* extract at different magnifications: (a) 5,000 $\times$ , (b) 20,000 $\times$ , (c) 100,000 $\times$  and (d) 200,000 $\times$ .

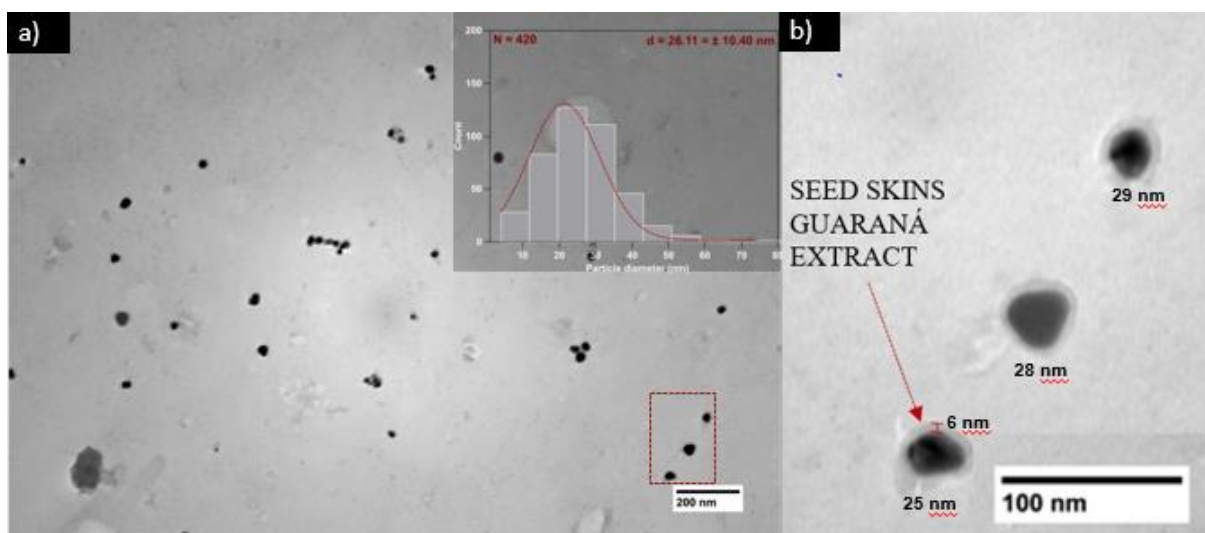


In SEM images recorded at high magnifications, it is evident the predominance of monodisperse AgNPs as well as a quasi-spherical shape which is consistent with TEM results. Similar results were obtained by Rodríguez-Félix et al. (2021) using an aqueous extract of *Carthamus tinctorius L.* as a source of capping/stabilizing extract. In their study, SEM images showed spherical AgNPs covered by the components present in the extract

TEM micrographs in Figure 23 exhibit the shape and size of the AgNPs successfully synthesized using guaraná extract.

Figure 23 - TEM micrographs of AgNPs obtained by green synthesis using *Paullinia Cupana* extract. a) AgNPs micrograph at 200 nm; b) Presence of guaraná seed skins extract; c)

Histogram of AgNPs.



Source: (Author, 2022)

It is evident from the TEM micrographs that AgNPs were quasi-spherical in shape, uniform in size distribution with particle size with diameter particle of 26,11( nm, which is less in size when compared to DLS values. This is expected because, in the DLS method, the hydrodynamic size is measured, which denotes the size of AgNPs with ions adsorbed on the surface, whereas TEM is performed using the dry particle. Still, some particles got agglomerated as can be seen in the micrograph and they were so neglected in calculating the size of AgNPs. Moreover, it is possible to see the capping agents such as alkaloids, proteins, and flavonoid compounds surrounding AgNPs, which is denoted by the presence of guaraná extracts in the reaction mixture.

The present data are in agreement with those of Khatamifar et al. (2021), who developed an eco-friendly, low-cost, and efficient method to synthesize AgNPs using *Quercus infectoria* extract as a source of reducing/stabilizing agents. Their results revealed that AgNPs were stable and their morphologies were spherical with an average diameter of 33 nm. In the same context, Prema et al. (2022) developed an optimization of AgNPs production using a central composite design with variable  $\text{AgNO}_3$  concentration, green tea extract, and temperature as factors. In their study, AgNPs were stably produced with an average diameter of 77 nm.

#### 4.3.6 Inductively coupled plasma atomic emission spectroscopy (ICP-OES)

The concentration of silver in the biosynthesized AgNPs in the colloidal solution was measured by ICP-OES. The concentration of silver in the AgNPs synthesized by seed skins guarná extract after 24h was found to be  $180 \pm 0.15$  ppm. This way, the yield of green synthesis was based on molar concentrations.

Taking in account that in the optimum condition was necessary to prepare 5 mM of  $\text{AgNO}_3$  to converter in AgNPs, 180 ppm of AgNPs was measured and the yield of reduction of  $\text{Ag}^+$  in the  $\text{Ag}^0$  was found to be 33.36%. Some phenomena can justify the low yield. Firstly,  $\text{Ag}^+$  ion might complex with compounds presents on the extract plant. Also, insufficient reducing/stabilizing agents and/or silver nitrate salt would be present in the green synthesis. Physical condition such as pH, temperature can influence on the bioreduction reaction (KUMAR, 2018)

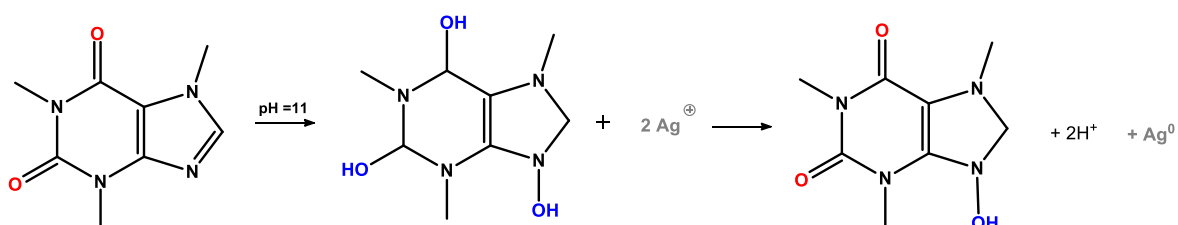
This results were higher than found by Almeida et al. (2017), who found 110 mg/L (110 ppm) using 1mM of silver nitrate concentration as metal precursor and *Fusarium oxysporum* as biologic agent. Also, El-Adawy et al. (2021) found  $10^4 \mu\text{g/mL}$  (ppm) using Gum-arabic as source of reducing/stabilizing agents. The difference between the yield of green synthesis found in the literature and this work is based on the interaction between the compounds present on the extract plant and the silver ion present in the colloidal solution.

#### 4.4 PROPOSED MECHANISM OF THE FORMATION OF SILVER NANOPARTICLES

A proposed chemical mechanism (Figure 24) for the silver ion to metallic silver nanoparticle was based on the majority compound present in the guaraná seed skins extract as shown by EM/SM results.

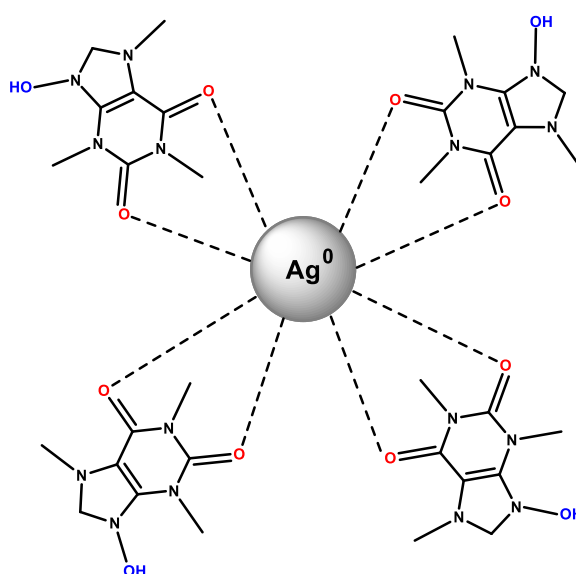
Figure 24 – Suggested mechanism for the silver ion to metallic silver nanoparticles via caffeine as reducing agent.

1,3,7-Trimethylxanthine  
(Caffeine)



Caffeine present in the guaraná seed skins extract in an alkaline medium (pH 11) may give electrons or hydrogen atoms with the constraints of carbon valency and the chelating action turn into quinone form (TELO, 1997). Silver ions are reduced by electrons to metallic silver in repeated times and aggregated in clusters of silver nanoparticles (Figure 25).

Figure 25 - Stabilization of silver nanoparticles performed by caffeine molecule present in the guaraná seed skins extract.





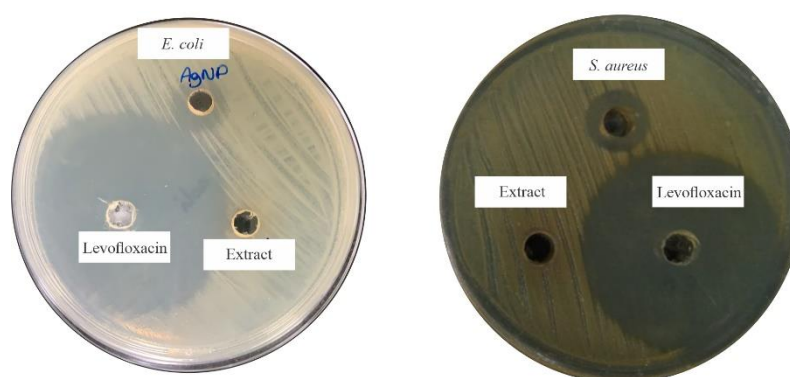
The reason why -OH band presents FTIR analysis decreases in intensity is justified when hydroxyl groups are used for reducing the silver ions. Therefore, it is suggested that caffeine plays an important role in the reduction/stabilizing of silver ions to produce silver nanoparticles.

It has been revealed that the performance in reduction of silver ion in silver nanoparticles depends upon the biomolecules present in the plant extracts. In most cases, macromolecules and phytochemicals such as catechins, flavonoids, ascorbic acids, alkaloids, proteins, and volatile acids are compounds responsible for reducing/stabilizing silver nanoparticles (RAJESHKUMAR, S., 2017). Nevertheless, when plant extracts are used in order to synthesize AgNPs, complex reactions can occur. Thus, the definitive mechanism is still open to discussion.

#### 4.3 ANTIBACTERIAL ACTIVITY OF SILVER NANOPARTICLES

AgNPs were tested to evaluate the antibacterial activity against gram-positive bacteria *S. aureus* and gram-negative bacteria *E. coli* were selected. Figure 26 shows the antibacterial activity of the biosynthesized AgNPs, seed skins extracts, and positive control (Levofloxacin) in the agar well diffusion method. The results were interpreted in terms of mean diameter as a zone of inhibition (ZOI) which is given in Table 11:

Figure 26. Antibacterial activity of biosynthesized AgNPs using seed skins extract against *E. coli* and *S. aureus*.



The seed skins extract did not show antibacterial activity for both bacterias tested. AgNPs exhibited significant antibacterial activity against *E. coli* and *S. aureus* in an AgNPs concentration of 100  $\mu\text{g/mL}$  with ZOI of  $15.7 \pm 0.4$  mm and  $13.3 \pm 0.2$  mm, respectively. Antibacterial activity of AgNPs revealed that *E. coli* is more susceptible when compared to *S. aureus*. This might be due to the difference in the bacterial cell wall structure (thickness of the peptidoglycan layer) which may prevent the action of silver ions. The cellular wall of *S. aureus* is composed of a thick layer of peptidoglycan while *E. coli* has an outer membrane with the structural lipopolysaccharide components which is narrower than *S. aureus* (YIN, 2020).

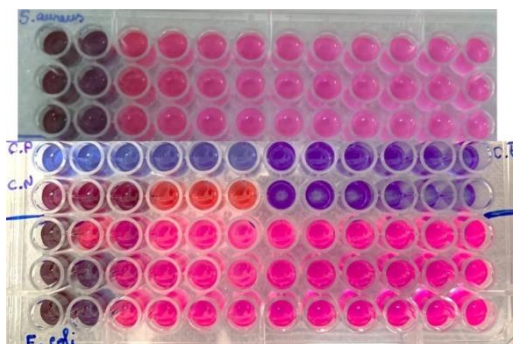
Table 11 - Inhibition zone (mm) of AgNPs using agar well diffusion method.

Bacteria	Inhibition zone (mm)		
	AgNPs (100 $\mu\text{g/mL}$ )	Guaraná seed skins extract (1% (m/v))	Levofloxacin (250 $\mu\text{g/mL}$ )
<i>Escherichia coli</i> (CCCD-E005)	15.7 $\pm$ 0.4	N/A	37.0 $\pm$ 0.6
<i>Staphylococcus aureus</i> (CCCD-S009)	13.3 $\pm$ 0.2	N/A	39.6 $\pm$ 0.4

Similar results were found by (DAS, 2018) in which AgNPs biosynthesized using leaf *Butea monosperma* (Lam.) extract exhibited good antibacterial activity by agar well diffusion method against *E. coli* and *S. aureus* with the zone of inhibition of  $9 \pm 1.2$  mm and  $7 \pm 1.0$  mm, respectively. Moreover, Raghava et al. (2021) synthesized AgNPs using *Rivina humilis* leaf extract with a concentration of  $100 \mu\text{g/mL}$ . In this case, it was also more efficient against *E. coli* than *S. aureus* with a zone of inhibition of  $7.5 \pm 0.04$  mm and  $4 \pm 0.05$  mm, respectively. The difference in the values of the zone of inhibition reported might be due to the size, shape, morphology, and/or stabilization of AgNPs.

The minimum inhibition concentration (MIC) for both bacteria *S. aureus* and *E. Coli* (Figure 27) were  $50 \mu\text{g/mL}$ . In both cases, it was found that AgNPs exhibit potential dose-dependent antibacterial activity. MIC values for *S. aureus* are similar to the results reported by He et al. (2017) using *Lotus* seeds extract for the synthesis of AgNPs achieving a MIC of  $20 \mu\text{g/mL}$  for *S. Aureus* as well as for *E. Coli*. In this case, the AgNPs were quasi-spherical with an average diameter of  $12.6 \pm 3.7$  nm in size.

Figure 27 - Determination of minimum inhibitory concentration (MIC) of AgNPs after 24h against *S. aureus* and *E. coli*.



The exact mechanism of bacterial actions of AgNPs is still not fully understood. Indeed, many possible mechanisms of action have been reported when AgNPs are involved (CHATTERJEE, 2015). The bacterial activity of AgNPs might be to the generation of the silver ions released which can act on the bacterial wall. Still, it was proposed that AgNPs could destroy the stability of the outer membrane of *E. Coli* which facilitates binding to the lower part of the peptidoglycan structure (DURAN, 2010). Also, some studies suggest that AgNPs can release silver ions and these ions can interact with thiol groups present in proteins and inactivate them (MATHEW, 2020). Besides, the antibacterial activity might be associated with characteristics shown by TEM images that reveal a small size of  $26 \pm 10$  nm in quasi-spherical shape.

Therefore, taking into account the antibacterial activity reported by literature and in this work, AgNPs can be confirmed as antibacterial agents.

## 5. CONCLUSIONS AND PERSPECTIVES

AgNPs were successfully synthesized using guaraná seed skin extracts as a source of reducing/stabilizing agents. A Taguchi experimental design enabled the optimization of the synthesis parameters so that AgNPs with a size of 26.11 nm and zeta potential of -11.2 mV were obtained. Moreover, an analysis of variance indicated that pH was the most important factor to influence the reduction reaction of ion silver.

The molecule of caffeine was detected as the major compound in the guaraná seed skins extract by DI-ESI-MS. Moreover, the main compounds measured as oxides in the guaraná seed skins powder, as detected by XRF, were potassium oxide (K<sub>2</sub>O), calcium oxide (CaO), and silicon dioxide (SiO<sub>2</sub>), respectively.

The formation of AgNPs and flavonoid compounds were detected by UV-Vis in the extract and AgNPs exhibited good stability after 30 days. Also, AgNPs were identified by XRD through typical peaks and some residues from the extract were also observed. Functional groups such as alkaloids, polyphenols, and flavonoids were observed by FTIR. These compounds were appointed as possible reducing/stabilizing agents. Quasi-spherical and monodisperse silver nanoparticles were observed by SEM/TEM. The TEM average size of AgNPs was lower than that measured by DLS due to the difference in measurement techniques. Using DLS, a negative charge was identified on the surface of silver nanoparticles probably due to the presence of OH<sup>-</sup>, COO<sup>-</sup>, and CO<sup>-</sup> groups. Also, ICP-OES detected a high concentration of 180 ppm as  $180 \pm 0.15$  ppm in the final solution of silver AgNPs. The proposed mechanism exhibited caffeine as a possible molecule that acted as stabilizing/reducing agent.

The antibacterial activity was effective in gram-positive (*S. aureus*) and gram-negative (*E. coli*) bacteria. *E. coli* ( $15.7 \pm 0.4$  mm) exhibited lower resistance than *S. aureus* ( $13.3 \pm 0.2$  mm) using the well-agar diffusion method. In broth microdilution, both exhibited the same MIC (50 µg/mL). In addition, the positive control revealed more resistance when compared with AgNPs. Guaraná seed skins extract did not show any antibacterial activity at 1% (m/v)..

Thus, the optimization of the green synthesis route using guaraná seed skins extract as a source of stabilizing/reducing agents is a sustainable alternative to traditional chemical methods to produce stable, monodisperse, and efficient AgNPs.

Further studies are suggested:

- Use of techniques such as High-Performance Liquid Chromatography (HPLC) to quantify the composition of guaraná seed skin extract with standards;
- Selection of more processing parameters (Type of extract, time of incubation, agitation) to achieve more robust data;
- Study of the influence of the anatomic plant structure to verify the influence on the reduction reaction;
- Selection of other response variables such as yield and/or stabilization (zeta potential).

## REFERENCES

ABDALLAH, B. M.; ALI, E. M. Green Synthesis of Silver Nanoparticles Using the *Lotus lalambensis* Aqueous Leaf Extract and Their Anti-Candidal Activity against Oral Candidiasis. **ACS Omega**, v. 6, n. 12, p. 8151-8162, 2021.

AHMAD, S. A. et al. Bactericidal activity of silver nanoparticles: a mechanistic review. **Materials Science for Energy Technologies**, 2020.

AHMED, S. et al. Green synthesis of silver nanoparticles: Antimicrobial potential and chemosensing of a mutagenic drug nitrofurazone in real samples. **Measurement**, v. 180, p. 109489, 2021.

ALEXANDER, J. W. History of the medical use of silver. **Surgical Infections**, v. 10, n. 3, p. 289-292, 2009.

ALMEIDA, Édipo da Silva. Biossíntese e caracterização de nanopartículas de prata por fusarium oxysporum. Dissertação de Mestrado. Florianópolis, SC, UFSC, 2017.

ALOMAR, T. S. et al. An eco-friendly plant-mediated synthesis of silver nanoparticles: Characterization, pharmaceutical and biomedical applications. **Materials Chemistry and Physics**, v. 249, p. 123007, 2020.

ALSUBKI, R. et al. Green synthesis, characterization, enhanced functionality and biological evaluation of silver nanoparticles based on *Coriander sativum*. **Saudi Journal of Biological Sciences**, v. 28, n. 4, p. 2102-2108, 2021.

ANANDALAKSHMI, K. et al. Green Synthesis, Characterization and Antibacterial Activity of Silver Nanoparticles Using *Chenopodium Album* Leaf Extract. **Indian Journal of Pure & Applied Physics (IJPAP)**, v. 59, n. 6, p. 456-461, 2021.

ANJU, T. R. et al. Green synthesis of silver nanoparticles from *Aloe vera* leaf extract and its antimicrobial activity. **Materials Today: Proceedings**, v. 43, p. 3956-3960, 2021.

ANTUNES, P. B. **Análise comparativa das frações polpa, casca, semente e pó comercial do guaraná (Paullinia cupana): caracterização química e atividade antioxidante in vitro**. 2011. Tese de Doutorado. Universidade de São Paulo.

BALACHANDRAN, Y. L. et al. Size-controlled green synthesis of silver nanoparticles using dual functional plant leaf extract at room temperature. **International Journal of Green Nanotechnology**, v. 4, n. 3, p. 310-325, 2012.

BALASHANMUGAM, P. ; KALAICHELVAN, P. T. Biosynthesis characterization of silver nanoparticles using *Cassia roxburghii* DC. aqueous extract, and coated on cotton cloth for effective antibacterial activity. **International Journal of Nanomedicine**, v. 10, n. Suppl 1, p. 87, 2015.

BARBOSA, V. T. et al. Síntese biogênica de nanopartículas de silver usando própolis vermelha de Alagoas. 2018.

BAXTER, P. J. et al. Cristobalite in volcanic ash of the soufriere hills volcano, montserrat, british west indies. **Science**, v. 283, n. 5405, p. 1142-1145, 1999.

BIANCO, Giuliana et al. Identification and fragmentation pathways of caffeine metabolites in urine samples via liquid chromatography with positive electrospray ionization coupled to a hybrid quadrupole linear ion trap (LTQ) and Fourier transform ion cyclotron resonance mass spectrometry and tandem mass spectrometry. **Rapid Communications in Mass Spectrometry: An International Journal Devoted to the Rapid Dissemination of Up-to-the-Minute Research in Mass Spectrometry**, v. 23, n. 7, p. 1065-1074, 2009.

BINDHU, M. R.; UMADEVI, M. Silver and gold nanoparticles for sensor and antibacterial applications. **Spectrochimica Acta Part A: Molecular and Biomolecular Spectroscopy**, v. 128, p. 37-45, 2014.

BISWAL, S. K. et al. Green Synthesis of Silver Nanoparticles Using Raw Fruit Extract of *Mimusops Elengi* and Their Antimicrobial Study. **Biointerface Res. Appl. Chem**, v. 11, p. 10040-10051, 2021.

BOGAS, A. C. et al. Endophytic bacterial diversity in the phyllosphere of Amazon *Paullinia cupana* associated with asymptomatic and symptomatic anthracnose. **Springerplus**, v. 4, n. 1, p. 1-13, 2015.

BURDUŞEL, A. et al. Biomedical applications of silver nanoparticles: an up-to-date overview. **Nanomaterials**, v. 8, n. 9, p. 681, 2018.



CARDOSO, M. L. C. **Desenvolvimento de metodologias analítica e tecnológica na obtenção de extratos secos nebulizados de *Heteropteris aphrodisiaca* O. Mach.-Malpighiaceae. Araraquara**, 128p. 2002. Tese de Doutorado.

CEYLAN, R. et al. Green synthesis of silver nanoparticles using aqueous extracts of three *Sideritis* species from Turkey and evaluations bioactivity potentials. **Sustainable Chemistry and Pharmacy**, v. 21, p. 100426, 2021.

CHAHARDOLI, A. et al. Green approach for synthesis of gold nanoparticles from *Nigella arvensis* leaf extract and evaluation of their antibacterial, antioxidant, cytotoxicity and catalytic activities. **Artificial cells, Nanomedicine and Biotechnology**, v. 46, n. 3, p. 579-588, 2018.

CHATTERJEE, T. et al. Antibacterial effect of silver nanoparticles and the modeling of bacterial growth kinetics using a modified Gompertz model. **Biochimica et Biophysica Acta (BBA)-General Subjects**, v. 1850, n. 2, p. 299-306, 2015.

CHOWDHURY, R. A. et al. Green synthesis and characterization of silver nanoparticles from the aqueous extract of the leaves of *Citrus aurantifolia*. **Materials Today: Proceedings**, v. 44, p. 1039-1042, 2021.

CLINICAL AND LABORATORY STANDARDS INSTITUTE – CLSI. Reference Method for Broth Dilution Antifungal Susceptibility Testing of Yeasts. M27, 4 ed, 2017.

CONAB. Companhia Nacional de Abastecimento. Conjuntura Mensal: Guaraná. Análise mensal outubro 2019. Retrieved from: <https://www.conab.gov.br/info-agro/analises-do-mercado-agropecuario-e-extrativista/analises-do-mercado/historico-mensal-de-Guaraná>. Accessed: February 01, 2022.

DAKAL, T. C. et al. Mechanistic basis of antimicrobial actions of silver nanoparticles. **Frontiers in Microbiology**, v. 7, p. 1831, 2016.

DAS, M.; SMITA, S. S. Biosynthesis of silver nanoparticles using bark extracts of *Butea monosperma* (Lam.) Taub. and study of their antimicrobial activity. **Applied Nanoscience**, v. 8, n. 5, p. 1059-1067, 2018.

DE MARIA, C. A; MOREIRA, R. F. Cafeína: revisão sobre métodos de análise. **Química Nova**, v. 30, p. 99-105, 2007.

DHAR, S. A. et al. Plant-mediated green synthesis and characterization of silver nanoparticles using *Phyllanthus emblica* fruit extract. **Materials Today: Proceedings**, v. 42, p. 1867-1871, 2021.

DOLEZ, P. I. Nanomaterials definitions, classifications, and applications. In: **Nanoengineering**. Elsevier, 2015. p. 3-40.

DTU Environment, 2021. The Nanodatabase Project. Available at: <<  
<http://nanodb.dk/en/>>>. Accessed on January 22, 2021.

DUANGJAI, Acharaporn et al. Comparison of antioxidant, antimicrobial activities and chemical profiles of three coffee (*Coffea arabica L.*) pulp aqueous extracts. **Integrative Medicine Research**, v. 5, n. 4, p. 324-331, 2016.

DUCKE, A. Diversidade dos guaranáis. **Rodriguésia**, v. 3, p.155-159, 1937.

DURAN, Ne. et al. Potential use of silver nanoparticles on pathogenic bacteria, their toxicity and possible mechanisms of action. **Journal of the Brazilian Chemical Society**, v. 21, n. 6, p. 949-959, 2010.

DUTTA, T. et al. Green synthesis of antibacterial and antifungal silver nanoparticles using *Citrus limetta* peel extract: Experimental and theoretical studies. **Journal of Environmental Chemical Engineering**, v. 8, n. 4, p. 104019, 2020.

DUVAL, R. E.; GOUYAU, J.; LAMOUREUX, E. Limitations of recent studies dealing with the antibacterial properties of silver nanoparticles: Fact and opinion. **Nanomaterials**, v. 9, n. 12, p. 1775, 2019.

EL-ADAWY, Mahmoud M. et al. Green synthesis and physical properties of Gum Arabic-silver nanoparticles and its antibacterial efficacy against fish bacterial pathogens. **Aquaculture Research**, v. 52, n. 3, p. 1247-1254, 2021.

EMBRAPA. Sistemas de produção 2. Cultura do Guaranázeiro no Amazonas (4. ed.). Novembro, 2005.

EMBRAPA. Empresa Brasileira de Pesquisa Agropecuária. UEPAE/Manaus. **1º Simpósio Brasileiro do Guaraná. Estado do Amazonas**. Anais. Manaus, EMBRAPA-UEPAE de Manaus, 1984.

ESFANDDARANI, H. M.; KAJANI, A. A.; BORDBAR, A. Green synthesis of silver nanoparticles using flower extract of *Malva sylvestris* and investigation of their antibacterial activity. **IET Nanobiotechnology**, v. 12, n. 4, p. 412-416, 2018.

European Commission. Commission recommendation of 18 October 2011 on the definition of nanomaterial. Off J Eur Union 2011;L 275:38e40

FIGUEROA, A. L. G. Guaraná, a máquina do tempo dos Sateré-Mawé. **Boletim do Museu Paraense Emílio Goeldi. Ciências Humanas**, v. 11, n. 1, p. 55-85, 2016

GOMES, E. B. Análise do comportamento da soldagem por Curto-Circuito aplicado ao processo Eletrodo Tubular através da Metodologia Taguchi. **Universidade Federal de Itajuba**, v. 99, 2006.

GRAÇA, R. *Licaria puchury-major (MART.) kosterm*: biossíntese de nanopartículas de silver dos extratos vegetais com atividade antimicrobiana. 2015.

GUARANÁ. **Pesquisa escolar online**, Fundação Joaquim Nabuco, Recife. Disponível em: < <http://basilio.fundaj.gov.br/pesquisaescolar/>>

GUIA GEOGRÁFICO. Guia geográfico do Amazonas. Available in : <https://www.brasil-turismo.com/amazonas.htm>; Accessed in February, 22, 2022.

GUIDANCE, D. Considering Whether an FDA-Regulated Product Involves the Application of Nanotechnology. 2011.

HAGGAG, E. G. et al. Antiviral potential of green synthesized silver nanoparticles of *Lampranthus coccineus* and *Malephora lutea*. **International Journal of Nanomedicine**, v. 14, p. 6217, 2019.

HE, Y. et al. Green synthesis of silver nanoparticles using seed extract of *Alpinia katsumadai*, and their antioxidant, cytotoxicity, and antibacterial activities. **RSC Advances**, v. 7, n. 63, p. 39842-39851, 2017.

HTWE, Y. Z. N. et al. Effect of silver nitrate concentration on the production of silver nanoparticles by green method. **Materials Today: Proceedings**, v. 17, p. 568-573, 2019

IBRAHIM, S. et al. Optimization for biogenic microbial synthesis of silver nanoparticles through response surface methodology, characterization, their antimicrobial, antioxidant, and catalytic potential. **Scientific Reports**, v. 11, n. 1, p. 1-18, 2021.

KAKAKHEL, M. A. et al. Green synthesis of silver nanoparticles and their shortcomings, animal blood a potential source for silver nanoparticles: A review. **Journal of Hazardous Materials Advances**, v. 1, p. 100005, 2021.

KANCHI, S; AHMED S. **Green metal nanoparticles: synthesis, characterization and their applications**. John Wiley & Sons, 2018.

KATTA, V. K. M.; DUBEY, R. S. Green synthesis of silver nanoparticles using *Tagetes erecta* plant and investigation of their structural, optical, chemical and morphological properties. **Materials Today: Proceedings**, v. 45, p. 794-798, 2021.

KAVITHA, M. et al. Green synthesis of silver nanoparticles using *Biophytum sensitivum* extract and its electrocatalytic activity towards dioxygen reduction. **Materials Today: Proceedings**, 2021.

KHALIL, M. MH et al. Green synthesis of silver nanoparticles using *olive* leaf extract and its antibacterial activity. **Arabian Journal of Chemistry**, v. 7, n. 6, p. 1131-1139, 2014.

KHATAMIFAR, M. et al. Green and eco-friendly synthesis of silver nanoparticles by *Quercus infectoria* galls extract: thermal behavior, antibacterial, antioxidant and anticancer properties. **Particulate Science and Technology**, p. 1-9, 2021.

KIM, S. M. et al. Optimization of parameters for the synthesis of bimodal Ag nanoparticles by Taguchi method. **Journal of Industrial and Engineering Chemistry**, v. 15, n. 6, p. 894-897, 2009.

KUMAR, B. et al. Extracellular green synthesis of silver nanoparticles using Amazonian fruit Araza (*Eugenia stipitata McVaugh*). **Transactions of Nonferrous Metals Society of China**, v. 26, n. 9, p. 2363-2371, 2016.

KUMAR, B. et al. Fabrication of silver nanoplates using *Nephelium lappaceum* (Rambutan) peel: a sustainable approach. **Journal of Molecular Liquids**, v. 211, p. 476-480, 2015.

KUMAR, S. V. et al. High conversion synthesis of < 10 nm starch-stabilized silver nanoparticles using microwave technology. **Scientific reports**, v. 8, n. 1, p. 1-10, 2018.

JADHAV, K. et al. Green and ecofriendly synthesis of silver nanoparticles: characterization, biocompatibility studies and gel formulation for treatment of infections in burns. **Journal of Photochemistry and Photobiology B: Biology**, v. 155, p. 109-115, 2016.

JAHANGIRIAN, H. et al. A review of drug delivery systems based on nanotechnology and green chemistry: green nanomedicine. **International journal of nanomedicine**, v. 12, p. 2957, 2017.

JAIN, S.; MEHATA, M. S. Medicinal plant leaf extract and pure flavonoid mediated green synthesis of silver nanoparticles and their enhanced antibacterial property. **Scientific Reports**, v. 7, n. 1, p. 1-13, 2017.

JEMILUGBA, O. T. et al. Green synthesis of silver nanoparticles using *Combretum erythrophyllum* leaves and its antibacterial activities. **Colloid and Interface Science Communications**, v. 31, p. 100191, 2019.

JIANG, X. C. et al. Role of temperature in the growth of silver nanoparticles through a synergetic reduction approach. **Nanoscale Res Lett**, v. 6, n. 1, p. 32, 2011.

JOHN, A. et al. Anti-bacterial and biocompatibility properties of green synthesized silver nanoparticles using *Parkia biglandulosa* (Fabales: Fabaceae) leaf extract. **Current Research in Green and Sustainable Chemistry**, p. 100112, 2021.

LAKSHMANAN, G. et al. Plant-mediated synthesis of silver nanoparticles using fruit extract of *Cleome viscosa L.*: assessment of their antibacterial and anticancer activity. **Karbala International Journal of Modern Science**, v. 4, n. 1, p. 61-68, 2018.

LEDO, A. da S. Potencialidade da fruticultura no estado do Acre. **Embrapa Acre-Documentos (INFOTECA-E)**, 1996.

LEE, S. et al. Effect of temperature on the growth of silver nanoparticles using plasmon-mediated method under the irradiation of green LEDs. **Materials**, v. 7, n. 12, p. 7781-7798, 2014.

LEON, L.; CHUNG, E.; RINALDI, C. A brief history of nanotechnology and introduction to nanoparticles for biomedical applications. **Nanoparticles for Biomedical Applications**. Elsevier, 2020. p. 1-4.

LIU, A. et al. Detection, characterization and identification of phenolic acids in Danshen using high-performance liquid chromatography with diode array detection and electrospray ionization mass spectrometry. **Journal of Chromatography A**, v. 1161, n. 1-2, p. 170-182, 2007.

LI, P. et al. Group IV nanodots: newly emerging properties and application in biomarkers sensing. **TrAC Trends in Analytical Chemistry**, p. 116007, 2020.

LI, W. et al. Antimicrobial activity of silver nanoparticles synthesized by the leaf extract of *Cinnamomum camphora*. **Biochemical Engineering Journal**, v. 172, p. 108050, 2021.

LIU, H. et al. Effect of temperature on the size of biosynthesized silver nanoparticle: deep insight into microscopic kinetics analysis. **Arabian Journal of Chemistry**, v. 13, n. 1, p. 1011-1019, 2020.

LORENZ, S. S. **Sateré-Mawé: os filhos do guaraná**. Coleção Projetos, volume 1. São Paulo: Centro de Trabalhados Indigenista, 1992.

LORENZI, H.; MATOS, F. **Plantas Medicinais do Brasil: nativas e exóticas cultivadas**. Nova Odessa: Instituto Plantarum, 2002.

MACHADO, K. N. et al. TNF- $\alpha$  inhibition, antioxidant effects and chemical analysis of extracts and fraction from Brazilian guaraná seed powder. **Food Chemistry**, v. 355, p. 129563, 2021.

MAHMOUD, M. G. et al. Facile green silver nanoparticles synthesis to promote the antibacterial activity of cellulosic fabric. **Journal of Industrial and Engineering Chemistry**, v. 99, p. 224-234, 2021.

MAIA, E. S. et al. Composição química e benefícios nutricionais dos caroços de açaí (*Euterpe precatória*), guaraná (*Paulinia cupana*) e tucumã (*Astrocaryum aculeatum*) na alimentação animal. 2022.

MAJHENIC, L.; ŠKERGET, M.; KNEZ, Ž. Antioxidant and antimicrobial activity of guaraná seed extracts. **Food Chemistry**, v. 104, n. 3, p. 1258-1268, 2007.

MALI, S. C. et al. Green synthesis of copper nanoparticles using *Celastrus paniculatus* Willd. leaf extract and their photocatalytic and antifungal properties. **Biotechnology Reports**, v. 27, p. e00518, 2020.

MANIKANDAN, D. B. et al. Green fabrication, characterization of silver nanoparticles using aqueous leaf extract of *Ocimum americanum* (Hoary Basil) and investigation of its in vitro antibacterial, antioxidant, anticancer and photocatalytic reduction. **Journal of Environmental Chemical Engineering**, v. 9, n. 1, p. 104845, 2021.

MANIK, U. P. et al. Green synthesis of silver nanoparticles using plant leaf extraction of *Artocarpus heterophyllus* and *Azadirachta indica*. **Results in Materials**, v. 6, p. 100086, 2020.

MARQUES, L. **Investigações fitoquímica e biológicas de extratos obtidos por tecnologia supercrítica de sementes de *Paullinia cupana* (guaraná)**. 2016. PhD thesis. State University of Maringá

MARQUES, L.L.M. et al. *Paullinia cupana*: a multipurpose plant – a review. **Revista Brasileira de Farmacognosia**, v. 29, n. 1, p. 77-110, 2019.

MARSLIN, G. et al. Antimicrobial activity of cream incorporated with silver nanoparticles biosynthesized from *Withania somnifera*. **International Journal of Nanomedicine**, v. 10, p. 5955, 2015.

MATHEW, S. et al. Biosynthesis of silver nanoparticle using flowers of *Calotropis gigantea* (L.) WT Aiton and activity against pathogenic bacteria. **Arabian Journal of Chemistry**, v. 13, n. 12, p. 9139-9144, 2020.

MCLELLAN, Tom M.; LIEBERMAN, Harris R. Do energy drinks contain active components other than caffeine?. **Nutrition reviews**, v. 70, n. 12, p. 730-744, 2012.

MELKAMU, W. W.; BITEW, L. T. Green synthesis of silver nanoparticles using *Hagenia abyssinica* (Bruce) JF Gmel plant leaf extract and their antibacterial and anti-oxidant activities. **Heliyon**, v. 7, n. 11, p. e08459, 2021.

MICHILES, R. J. et al. **A cadeia produtiva do guaraná: um estudo com o guaraná no município de Maués**. 2010.

MIRI, A. et al. Plant-mediated biosynthesis of silver nanoparticles using *Prosopis farcta* extract and its antibacterial properties. **Spectrochimica Acta Part A: Molecular and Biomolecular Spectroscopy**, v. 141, p. 287-291, 2015.

MONTAZER, M.; SHAMEI, A.; ALIMOHAMMADI, F. Synthesizing and stabilizing silver nanoparticles on polyamide fabric using silver-ammonia/PVP/UVC. **Progress in Organic Coatings**, v. 75, n. 4, p. 379-385, 2012

MONTGOMERY, D. C. **Statistical quality control**. Wiley Global Education, 2012.

MORTAZAVI-DERAZKOLA, S. et al. Green Synthesis and Investigation of Antibacterial Activity of Silver Nanoparticles Using *Eryngium bungei* Boiss Plant Extract. **Journal of Polymers and the Environment**, 2021.

MORTAZAVI-DERAZKOLA, S. et al. Green Synthesis and Characterization of Silver Nanoparticles Using *Elaeagnus angustifolia* Bark Extract and Study of Its Antibacterial Effect. **Journal of Polymers and the Environment**, 2021.

MUNIYAPPAN, N.; NAGARAJAN, N. S. Green synthesis of silver nanoparticles with *Dalbergia spinosa* leaves and their applications in biological and catalytic activities. **Process Biochemistry**, v. 49, n. 6, p. 1054-1061, 2014

MUTHUKRISHNAN, S. et al. Biosynthesis, characterization and antibacterial effect of plant-mediated silver nanoparticles using *Ceropegia thwaitesii*—An endemic species. **Industrial crops and products**, v. 63, p. 119-124, 2015.

NAAZ, R. et al. Green synthesis of silver nanoparticles using *Syngonium podophyllum* leaf extract and its antibacterial activity. **Materials Today: Proceedings**, 2021.



OVAIS, M. et al. Current state and prospects of the phytosynthesized colloidal gold nanoparticles and their applications in cancer theranostics. **Applied Microbiology and Biotechnology**, v. 101, n. 9, p. 3551-3565, 2017.

PALITHYA, S. et al. Green synthesis of silver nanoparticles using flower extracts of *Aerva lanata* and their biomedical applications. **Particulate Science and Technology**, p. 1-13, 2021.

PAREEK, V.; GUPTA, R.; PANWAR, J. Do physico-chemical properties of silver nanoparticles decide their interaction with biological media and bactericidal action? A review. **Materials Science and Engineering: C**, v. 90, p. 739-749, 2018.

PATINO-RUIZ, D. et al. Green synthesis of iron oxide nanoparticles using *Cymbopogon citratus* extract and sodium carbonate salt: Nanotoxicological considerations for potential environmental applications. **Environmental Nanotechnology, Monitoring & Management**, v. 14, p. 100377, 2020.

PAUL, M.; LONDHE, V. Y. *Pongamia pinnata* seed extract-mediated green synthesis of silver nanoparticles: Preparation, formulation and evaluation of bactericidal and wound healing potential. **Applied Organometallic Chemistry**, v. 33, n. 3, p. e4624, 2019.

PEIXOTO, H. et al. Anti-aging and antioxidant potential of *Paullinia cupana* var. *sorbilis*: Findings in *Caenorhabditis elegans* indicate a new utilization for roasted seeds of guaraná. **Medicines**, v. 4, n. 3, p. 61, 2017.

PINHO, L. S. et al. Guaraná (*Paullinia cupana*) by-product as a source of bioactive compounds and as a natural antioxidant for food applications. **Journal of Food Processing and Preservation**, v. 45, n. 10, p. e15854, 2021.

POH, T. Y. et al. Inhaled nanomaterials and the respiratory microbiome: clinical, immunological and toxicological perspectives. **Particle and Fibre Toxicology**, v. 15, n. 1, p. 1-16, 2018.

PREMA, P. et al. Statistical optimization of silver nanoparticle synthesis by green tea extract and its efficacy on colorimetric detection of mercury from industrial waste water. **Environmental Research**, v. 204, p. 111915, 2022.

PRINCY, K. F.; GOPINATH, A. Green synthesis of silver nanoparticles using polar seaweed *Fucus gardeneri* and its catalytic efficacy in the reduction of nitrophenol. **Polar Science**, p. 100692, 2021.

PROJETO Potencialidades Regionais: estudo de viabilidade econômica: guaraná. Manaus: ISAE/FGV: **Suframa**, 2003. 28 p.

QUE, Z. G. et al. Application of silver nanoparticles for water treatment. **IntechOpen**, 2018.

RAFIQUE, M. et al. History and fundamentals of nanoscience and nanotechnology. In: **Nanotechnology and Photocatalysis for Environmental Applications**. Elsevier, 2020. p. 1-25.

RAGHAVA, S.; MBAE, K. M.; UMESHA, S. Green synthesis of silver nanoparticles by *Rivina humilis* leaf extract to tackle growth of Brucella species and other perilous pathogens. **Saudi Journal of Biological Sciences**, v. 28, n. 1, p. 495-503, 2021.

RAJ, S.; TRIVEDI, R.; SONI, V. Biogenic Synthesis of Silver Nanoparticles, Characterization and Their Applications—A Review. **Surfaces**, v. 5, n. 1, p. 67-90, 2022.

RAJESHKUMAR, S.; BHARATH, L. V. Mechanism of plant-mediated synthesis of silver nanoparticles—a review on biomolecules involved, characterisation and antibacterial activity. **Chemico-biological interactions**, v. 273, p. 219-227, 2017.

RAMESH, A. V. et al. A Facile plant mediated synthesis of silver nanoparticles using an aqueous leaf extract of *Ficus hispida* Linn. f. for catalytic, antioxidant and antibacterial applications. **South African Journal of Chemical Engineering**, v. 26, p. 25-34, 2018.

RAMESH, P. S.; KOKILA, T.; GEETHA, D. Plant mediated green synthesis and antibacterial activity of silver nanoparticles using *Emblica officinalis* fruit extract. **Spectrochimica Acta Part A: Molecular and Biomolecular Spectroscopy**, v. 142, p. 339-343, 2015.

RANA, A.; YADAV, K.; JAGADEVAN, S. A comprehensive review on green synthesis of nature-inspired metal nanoparticles: Mechanism, application and toxicity. **Journal of Cleaner Production**, p. 122880, 2020.

RAUWEL, P. et al. A review on the green synthesis of silver nanoparticles and their morphologies studied via TEM. **Advances in Materials Science and Engineering**, v. 2015, 2015.

RAZA, M. A. et al. Size-and shape-dependent antibacterial studies of silver nanoparticles synthesized by wet chemical routes. **Nanomaterials**, v. 6, n. 4, p. 74, 2016.

RODRIGUES, G. et al. Can metallic nanomaterials be green and sustainable?. **Current Opinion in Environmental Science & Health**, v. 24, p. 100292, 2021.

RODRÍGUEZ-FÉLIX, F. et al. Sustainable-green synthesis of silver nanoparticles using safflower (*Carthamus tinctorius L.*) waste extract and its antibacterial activity. **Heliyon**, v. 7, n. 4, p. e06923, 2021.

SALEH, T.A. Nanomaterials: Classification, properties, and environmental toxicities, **Environmental Technology & Innovation**, v. 20, p. 101067, 2020.

SANTOS, F. S.; SARAIVA, JMV; ATROCH, A. L. Influência da precipitação pluvial na produtividade do guaraná no município de Maués, AM. 2021.

SELLAMI, M. et al. Herbal medicine for sports: a review. **Journal of the International Society of Sports Nutrition**, v. 15, n. 1, p. 1-14, 2018.

SHAIKH, W. A. et al. A review of the phytochemical mediated synthesis of AgNP (silver nanoparticle): the wonder particle of the past decade. **Applied nanoscience**, v. 11, n. 11, p. 2625-2660, 2021.

SHAKER ARDAKANI, L. et al. Silver nanoparticles (Ag NPs) as catalyst in chemical reactions. **Synthetic Communications**, v. 51, n. 10, p. 1516-1536, 2021.

SHARMA, R. K. et al. Silver nanomaterials: Synthesis and (electro/photo) catalytic applications. **Chemical Society Reviews**, 2021.

SIDDIQI, K. S.; HUSEN, A.I; RAO, R. AK. A review on biosynthesis of silver nanoparticles and their biocidal properties. **Journal of Nanobiotechnology**, v. 16, n. 1, p. 1-28, 2018.

SILVA, A. C. B. et al. Aliança guaraná de Maués: a cadeia de valor do guaraná de Maués. **Manaus: IDESAM**, 2018.

SILVA, L. Síntese verde de nanopartículas de prata com extrato aquoso de folhas de *Brosimum gaudichaudii*, caracterização físicoquímica, morfológica e suas aplicações no desenvolvimento de um nanobiossensor eletroquímico. 2014. 121 f., il. **Dissertação (Mestrado em Nanociência e Nanobiotecnologia)**—Universidade de Brasília, Brasília, 2014.

SILVA, M. P. et al. Production and characterization of solid lipid microparticles loaded with guaraná (*Paullinia cupana*) seed extract. **Food Research International**, v. 123, p. 144-152, 2019.

SILVERSTEIN, R. M.; BASSLER, G. C. Spectrometric identification of organic compounds. **Journal of Chemical Education**, v. 39, n. 11, p. 546, 1962.

SINGH, H; DU, J; YI, T. Green and rapid synthesis of silver nanoparticles using *Borago officinalis* leaf extract: anticancer and antibacterial activities. **Artificial Cells, Nanomedicine, and Biotechnology**, v. 45, n. 7, p. 1310-1316, 2017.

SINGH, J. et al. Study of structural, optical properties and antibacterial effects of silver nanoparticles synthesized by green synthesis method. **Materials Today: Proceedings**, 2021.

SLAVIN, Y. N. et al. Metal nanoparticles: understanding the mechanisms behind antibacterial activity. **Journal of Nanobiotechnology**, v. 15, n. 1, p. 1-20, 2017.

SOFI, M. A. et al. An overview of antimicrobial and anticancer potential of silver nanoparticles. **Journal of King Saud University-Science**, p. 101791, 2021.

SOMBRA, L. L. et al. Comparative study between capillary electrophoresis and high performance liquid chromatography in ‘guaraná’ based phytopharmaceuticals. **Journal of pharmaceutical and biomedical analysis**, v. 36, n. 5, p. 989-994, 2005. SUKWEENADHI, J. et al. Scale-up of green synthesis and characterization of silver nanoparticles using ethanol extract of *Plantago major L.* leaf and its antibacterial potential. **South African Journal of Chemical Engineering**, v. 38, p. 1-8, 2021.

SUMAN, T. Y. et al. Biosynthesis, characterization and cytotoxic effect of plant mediated silver nanoparticles using *Morinda citrifolia* root extract. **Colloids and surfaces B: Biointerfaces**, v. 106, p. 74-78, 2013.

**Superintendência da Zona Franca de Manaus**. Potencialidades Regionais: estudo da viabilidade econômica, Guaraná. Manaus: SUFRAMA, 2003.

TAN, T. B. et al. Physicochemical, morphological and cellular uptake properties of lutein nanodispersions prepared by using surfactants with different stabilizing mechanisms, **Food & Function**, v. 7, p. 2043-2051, 2016.

TELO, João P.; VIEIRA, Abel JSC. Mechanism of free radical oxidation of caffeine in aqueous solution. **Journal of the Chemical Society, Perkin Transactions 2**, n. 9, p. 1755-1758, 1997.

TER STEEGE, H. et al. The discovery of the Amazonian tree flora with an updated checklist of all known tree taxa. **Scientific Reports**, v. 6, n. 1, p. 1-15, 2016.

TRIPATHI, D. et al. Biomedical potential of green synthesized silver nanoparticles from root extract of *Asparagus officinalis*. **Journal of Plant Biochemistry and Biotechnology**, p. 1-6, 2021.

URNUKHSIAKHAN, E. et al. Antibacterial Activity and Characteristics of Silver Nanoparticles Biosynthesized From *Carduus Crispus*. **Research Square**. 2021.

VALENTE, A. **Modelação de um edifício e obtenção da solução ótima de climatização aplicando a metodologia de Taguchi**. 2017. Tese de Doutorado. Instituto Politécnico de Setúbal. Escola Superior de Tecnologia de Setúbal.

VARADAVENKATESAN, T.; VINAYAGAM, R.; SELVARAJ, R. Structural characterization of silver nanoparticles phyto-mediated by a plant waste, seed hull of Vigna mungo and their biological applications. **Journal of Molecular Structure**, v. 1147, p. 629-635, 2017.

VEGGI, P. **Obtenção de compostos fenólicos de plantas brasileiras via tecnologia supercrítica utilizando cossolventes e extração assistida por ultrassom**. 2013. 190 p. Tese

(doutorado) - Universidade Estadual de Campinas, Faculdade de Engenharia de Alimentos, Campinas, SP.

VLÂSCEANU, G. M. et al. Silver nanoparticles in cancer therapy. In: **Nanobiomaterials in Cancer Therapy**. William Andrew Publishing, 2016. p. 29-56.

WANG, Y. et al. Green synthesis and chemical characterization of a novel anti-human pancreatic cancer supplement by silver nanoparticles containing *Zingiber officinale* leaf aqueous extract. **Arabian Journal of Chemistry**, v. 14, n. 4, p. 103081, 2021.

YIN, I.X. et al. The antibacterial mechanism of silver nanoparticles and its application in dentistry. **International Journal of Nanomedicine**, v. 15, p. 2555, 2020.

ZHANG, X. et al. Silver nanoparticles: synthesis, characterization, properties, applications, and therapeutic approaches. **International Journal of Molecular Sciences**, v. 17, n. 9, p. 1534, 2016.